



University of Natural Resources
and Life Sciences, Vienna
Department of Chemistry

Expression, purification and functional
characterization of a heme-thiolate peroxygenase of
Aspergillus niger

Master thesis

Submitted by

Susanne Dachs

Vienna, February 2016

University of Natural Resources and Life Sciences, Vienna

Department of Chemistry, Division of Biochemistry

Protein Biochemistry Group

Danksagung

Danke an Christian Obinger, der es mir ermöglicht hat, meine Masterarbeit in der Arbeitsgruppe für Proteinbiochemie zu absolvieren.

Danke an Paul Furtmüller für die fachliche Unterstützung, die zahlreichen Erklärungen und die große Geduld.

Danke an die Arbeitsgruppe für Proteinbiochemie für die moralische Unterstützung und die schöne, lustige Zeit zusammen.

Danke an meine Eltern, meine Geschwister und meine Großeltern, die mich zu jeder Zeit und in jeglicher Hinsicht unterstützt haben.

Table of contents

Abstract	1
1 Introduction	3
1.1 Phylogenetics	3
1.1.1 Peroxidase-peroxygenase superfamily	4
1.1.2 Chloroperoxidase from <i>Caldariomyces fumago</i>	6
1.1.3 Unspecific peroxygenase from <i>Agrocybe aegerita</i>	6
1.2 Structure of peroxidase-peroxygenases	8
1.2.1 Heme structure	8
1.2.2 Active site residues in peroxidase-peroxygenases	9
1.3 Reaction mechanism of unspecific peroxygenase.....	11
1.4 Industrial applications of peroxidase-peroxygenases	12
2 Aim of the thesis.....	15
3 Materials and Methods.....	17
3.1 Transformation of <i>AnHTP</i> into <i>Pichia Pastoris</i> cells	17
3.1.1 Vector	17
3.1.2 Transformation of vector in <i>E. coli</i> cells	17
3.1.3 DNA purification	20
3.1.4 Transformation of linearized plasmid DNA in <i>Pichia</i> cells	20
3.2 Expression screening	23
3.3 Protein production	26
3.3.1 Sterile technique	26
3.3.2 Preparation of stock solutions.....	26
3.3.3 Preparation of media and buffers.....	27
3.3.4 Cultivation of cells.....	29
3.3.5 Harvesting of cells.....	29
3.4 Protein purification.....	30
3.4.1 Ammonium sulfate precipitation	30
3.4.2 Preparation of the supernatant.....	31
3.4.3 Immobilized Metal Ion Affinity chromatography.....	32
3.4.4 Desalting.....	35
3.5 Protein characterization.....	36
3.5.1 Spectral properties.....	36
3.5.2 Extinction coefficient determination.....	37

3.5.3	UV/vis spectrum.....	37
3.5.4	pH-dependency of the UV/vis spectrum.....	38
3.5.5	Reduction with sodium dithionite.....	38
3.5.6	SDS-PAGE	39
3.5.7	Western Blot	40
3.5.8	Steady-state kinetics.....	42
3.5.9	Sodium cyanide titration.....	49
3.5.10	Circular dichroism	50
3.5.11	Differential scanning calorimetry.....	51
3.5.12	Size-exclusion HPLC	52
3.5.13	Stopped-flow spectroscopy.....	53
4	Results and Discussion.....	55
4.1	Expression screening	55
4.2	Protein purification.....	56
4.3	Extinction coefficient determination	59
4.4	UV/vis spectrum	60
4.5	Size exclusion HPLC	62
4.6	pH-dependency of the UV/vis spectrum	64
4.7	Reduction with sodium dithionite	65
4.8	Steady-state kinetics	67
4.9	Sodium cyanide titration	73
4.10	Circular Dichroism	75
4.11	Differential Scanning Calorimetry	79
4.12	Stopped-flow spectroscopy	80
5	Conclusion	84
6	References.....	86

Abstract

There are four heme peroxidase superfamilies known to date. These enzymes use heme as redox cofactor to catalyze the hydrogen peroxide mediated one- and two-electron oxidation of substrate molecules such as aromatic molecules, cations, anions or even proteins. One of them is called the peroxidase–peroxygenase superfamily. In contrast to the other three superfamilies it is rarely investigated. Approximately one thousand putative fungal peroxidase-peroxygenase sequences can be found in genetic databases indicating a widespread occurrence of this enzyme. Peroxidase-peroxygenase uses hydrogen peroxide to introduce oxygen into organic molecules. This process is called oxyfunctionalization and it is unique among these enzymes.

In this thesis, the heme-thiolate peroxygenase from *Aspergillus niger* (AnHTP) was expressed in *Pichia pastoris*. The protein was characterized by a wide range of biochemical and biophysical methods. After ammonium sulfate precipitation and metal chelate affinity chromatography the highly glycosylated monomeric enzyme was purified to homogeneity with a yield of 2.8 mg/L. Using several substrates, the redox active enzyme shows both peroxidase and peroxygenase activity. Temperature stability was measured using circular dichroism and differential scanning calorimetry. Both methods showed an almost identical unfolding process with a single unfolding event. Compound I formation was analyzed with stopped-flow spectroscopy using the substrate *meta*-chloroperoxybenzoic acid (CPBA). Results were discussed in relation to the well characterized chloroperoxidase from *Caldariomyces fumago* and unspecific peroxygenase from *Agrocybe aegerita*.

Zusammenfassung

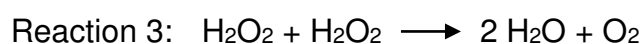
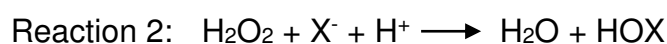
Bislang sind vier Häm-Peroxidase Superfamilien bekannt. Diese Enzyme verwenden Häm als Redox-Cofaktor für die Katalyse von Wasserstoffperoxid-medierten Ein- und Zwei-Elektronen-Oxidationsreaktionen von Substratmolekülen wie aromatischen Molekülen, Kationen, Anionen oder sogar Proteinen. Eine von diesen Superfamilien wird Peroxidase-Peroxygenase Superfamilie genannt. Im Gegensatz zu den anderen drei Superfamilien ist sie kaum untersucht. Etwa eintausend mutmaßliche Peroxidase-Peroxygenase Sequenzen aus Pilzen findet man in genetischen Datenbanken, was auf ein weit verbreitetes Vorkommen dieser Enzyme hindeutet. Peroxidase-Peroxygenasen verwenden Wasserstoffperoxid, um Sauerstoff in organische Moleküle einzubauen. Dieser Prozess wird Oxyfunktionalisierung genannt und ist einzigartig unter Enzymen.

In dieser Arbeit wurde die Hämthiolat-Peroxygenase aus *Aspergillus niger* (AnHTP) in *Pichia pastoris* exprimiert. Das Protein wurde mit einer breiten Auswahl an biochemischen und biophysikalischen Methoden charakterisiert. Nach einer Ammoniumsulfat-Fällung und einer Metallchelat-Affinitätschromatografie wurde das stark glykosylierte monomere Enzym mit einer Ausbeute von 2,8 mg/L homogen gereinigt. Mit unterschiedlichen Substraten zeigt das redoxaktive Enzym sowohl Peroxidase- als auch Peroxygenase-Aktivität. Die Temperaturstabilität wurde mittels Zirculardichroismus und dynamischer Differenzkalorimetrie gemessen. Beide Methoden zeigten einen fast identischen Entfaltungsprozess mit einem einzigen Entfaltungs-Übergang. Compound I-Bildung wurde mit Stopped-Flow Spektroskopie unter Verwendung des Substrates *meta*-Chlorperbenzoesäure (CPBA) analysiert. Die Ergebnisse wurden in Bezug auf die gut charakterisierte Chlorperoxidase aus *Caldaryomyces fumago* und der unspezifischen Peroxygenase aus *Agrocybe aegerita* diskutiert.

1 Introduction

1.1 Phylogenetics

Heme peroxidases (EC number 1.11.1.7) can be discovered in all living organisms. They catalyze one- and two-electron oxidations of multiple substrates with hydrogen peroxide as the electron acceptor. There are mainly four reaction types, that heme peroxidases are able to catalyze, which are shown below. In all of these reactions, a hydrogen peroxide molecule is reduced and turned into water. Reaction 1 describes the transition of one-electron donors AH_2 into their corresponding radicals $\cdot AH$. In reaction 2, two-electron donors like halides X^- are oxidized to their corresponding hypohalous acids HOX . Reaction 3 depicts the catalytic reaction, using a second hydrogen peroxide molecule as two-electron donor, which results in the release of an oxygen molecule. The peroxygenation reaction, shown in reaction 4, is only catalyzed by a certain group of heme peroxidases, the peroxidase-peroxygenases, which are described below. During peroxygenation, the oxygen from the hydrogen peroxide is selectively incorporated into organic molecules ROH (Zámocký et al., 2015).



The active site of heme peroxidases, where these reactions take place, contains heme *b* or posttranslationally modified heme as a cofactor. There are four heme peroxidase superfamilies that developed independently from each other during evolution: the peroxidase-catalase, the peroxidase-cyclooxygenase, the peroxidase-chlorite dismutase and the peroxidase-peroxygenase superfamily. Recently, these superfamilies were newly classified according to their sequence signature, essential amino acids in the

active site and typical activities. (Zámocký *et al.*, 2015). Among the four superfamilies, there are differences in oligomeric organization, monomer architecture, active site geometry and catalytic residues. (Zámocký *et al.*, 2012).

1.1.1 Peroxidase-peroxygenase superfamily

This enzyme family still consists of many putative sequences, therefore the phylogeny is not final yet. (Zámocký *et al.*, 2015) Peroxidase-peroxygenases occur mainly in fungi, particularly in the widespread branches of ascomycetes and basidiomycetes. Figure 1-1 shows a phylogenetic tree of 136 peroxidase-peroxygenase sequences.

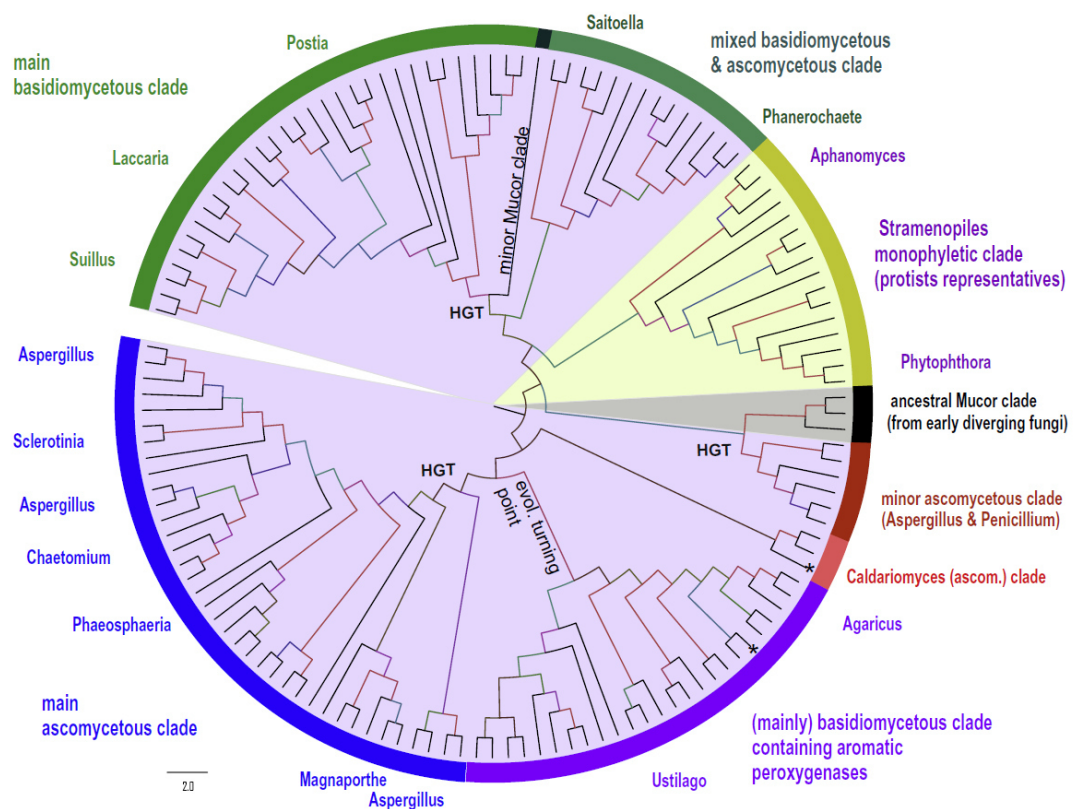


Figure 1-1: Phylogenetic tree of 136 members of the peroxidase-peroxygenase superfamily (Zámocký *et al.*, 2015), the two stars inside the circle marking CPO (upper) and UPO (lower)

The figure demonstrates that the first ancestors of peroxidase-peroxygenases already developed when the evolution of the fungal kingdom started. These were enzymes from the early evolving division Zygomycota called *Mucor* peroxidases.

Alongside the so called minor fungal enzymes with their well-known representative chloroperoxidase from *Caldariomyces fumago* (CPO), the clade of Stramenopiles developed rather early. In contrast to that, unspecific aromatic peroxygenases like the one from basidiomyceta *Auricularia delicata* (AaeAPO), diverged later in evolution from *Mucor* peroxidases. Because of differences in the heme pocket between AaeAPO and chloroperoxidase, the evolution of the minor clade (shown in figure 1-1) marks a turning point in the development of peroxidase-peroxygenases. The basidiomycetous and the ascomycetous clades still mainly contain completely putative sequences. That is why the physiological role and the enzymatic activity as well as the structure has to be elucidated (Zámocký *et al.*, 2015).

The peroxidase-peroxygenase superfamily is the least investigated, but the most unique heme peroxidase superfamily. There are several terms used in literature for enzymes from this family, namely heme-thiolate peroxidases (HTPs), unspecific peroxygenases (UPOs) or aromatic peroxygenases (APOs). They are secreted and highly glycosylated, therefore usually particularly stable (Hofrichter *et al.*, 2014). In contrast to all the other heme peroxidases, members of the peroxidase-peroxygenase superfamily possess a cysteine as proximal heme ligand instead of the usual histidine. This cysteine and its corresponding -X-Proline-Cysteine-Proline-X- motif are highly conserved among the members of the family. Whereas the catalytically active distal side shows a high inconstancy. Functionally, these enzymes are a mixture between peroxidases and P450-monooxygenases (Zámocký *et al.*, 2015). Moreover, they catalyze selective oxyfunctionalizations, reactions that are difficult to realize and desired for industrial applications. During oxyfunctionalization reactions, the oxygen from a hydrogen peroxide molecule is transferred into the reaction product. Hydroxylations, epoxidations, dealkylations, oxidations of organic hetero atoms and inorganic halides and one-electron oxidations belong to this kind of reactions (Hofrichter *et al.*,

2014). So far, only P450-monooxygenases are known to catalyze these reactions. P450-monooxygenases are structurally related to peroxidase-peroxygenases, because they also have a proximal cysteine ligand, which explains that both catalyze partly the same kind of reactions. But the big advantage of peroxidase-peroxygenases concerning so called oxyfunctionalization reactions is, that they don't need an additional regeneration enzyme system like P450 monooxygenases, because they use hydrogen peroxide directly as cosubstrate (Bormann *et al.*, 2015).

1.1.2 Chloroperoxidase from *Caldariomyces fumago*

Chloroperoxidase (CPO) is the best studied member of the peroxidase-peroxygenase superfamily. It has been under investigation for over 50 years (Bormann *et al.*, 2015) and for a long time it has been the only representative of this enzyme family. Its physiological role is to synthesize the antibiotic caldariomycin by catalyzing the chlorination of cyclopentanedione in the fungi *Caldariomyces fumago* (Kühnel *et al.*, 2006). Chloroperoxidase mainly catalyzes chlorination and bromination reactions, but it also has peroxygenase activity. However, it can only transfer oxygen from hydrogen peroxide to activated substrates. This is a constraint that unspecific peroxygenases do not have. They all catalyze hydrogen peroxide dependent non-activated C-H bond hydroxylations, also called oxyfunctionalizations, which is an outstanding advantage compared to chloroperoxidase (Hofrichter *et al.*, 2014). These kinds of reactions belong to the most important reactions in organic synthesis (Molina-Espeja *et al.*, 2014).

Because there is a lot of information available concerning structural and functional characterization, phylogenetically related chloroperoxidase was used for comparison with heme-thiolate peroxygenase from *Aspergillus niger* (AnHTP) in this thesis.

1.1.3 Unspecific peroxygenase from *Agrocybe aegerita*

Next to chloroperoxidase, unspecific peroxygenase (UPO), also called aromatic peroxygenase (APO) from *Agrocybe aegerita* has been studied

extensively in the last decade. Chloroperoxidase shows a 30 % sequence homology to UPO, which is higher than the homology of any other heme enzyme to unspecific peroxygenase (Piontek *et al.*, 2013). The physiological function of UPO is not fully elucidated yet, but it might play a role in transformation of lignin and humus, furthermore in detoxifying plant compounds (Molina-Espeja *et al.*, 2014). UPO is a versatile biocatalyst, catalyzing the in chapter 1.1.1 mentioned oxyfunctionalization reactions. Hydroxylation of alkanes by UPO, for example, achieves an enantioselectivity, far greater than that of P450-monoxygenases. It also has a halogenating activity, however it is far less high than the activity of chloroperoxidase. There is a long list of substrates, it is able to catalyze (a selection is depicted in figure 1-2): halides, toluene, ethylbenzene, saturated and unsaturated fatty acids, N- and S- oxidation of heterocycles, cleavage of ethers (Hofrichter *et al.*, 2010).

UPO was used for comparison as well as chloroperoxidase, because it is related to AnHTP and there are various data available.

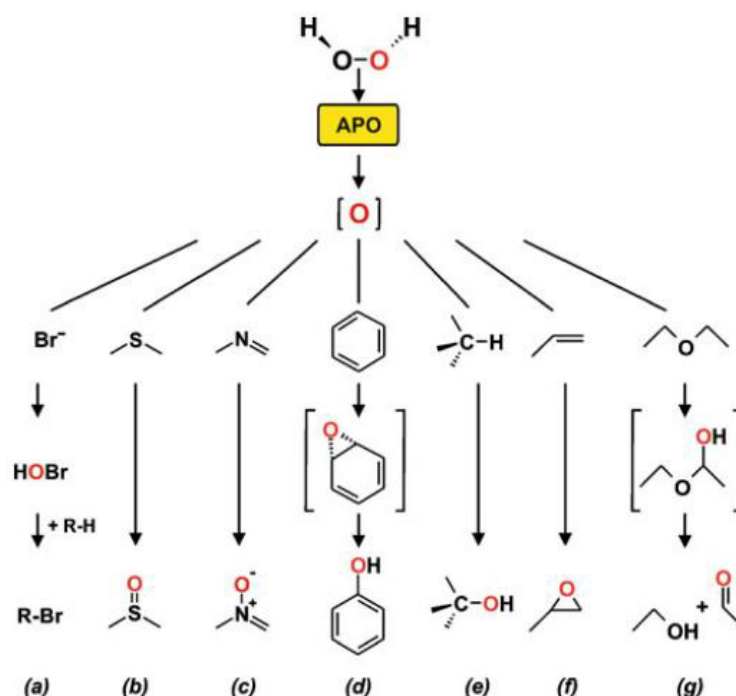


Figure 1-2: Reactions catalyzed by aromatic peroxygenase (APO, also called UPO): a) Bromination, b) Sulfoxidation, c) N-oxidation, d) Aromatic peroxygenation, e) Alkyl hydroxylation, f) Double bond epoxidation, g) Ether cleavage (Hofrichter *et al.*, 2010)

1.2 Structure of peroxidase-peroxygenases

There are two crystal structures of peroxidase-peroxygenases known up to now. One of them is chloroperoxidase and the other one is the structure of UPO from *Agrocybe aegerita*. Peroxidase-peroxygenases possess a heme *b* in their active site, which is the crucial structure for the enzymatic activity of these enzymes.

1.2.1 Heme structure

Heme *b* (shown in figure 1-3), consisting of protoporphyrin IX and an iron atom in the center, is the prosthetic group in most of the heme enzymes. Protoporphyrin IX is an organic chemical compound composed of four pyrrol rings connected to each other by methine bridges. Four methyl groups, two vinyl groups and two propionate side chains are bound to the protoporphyrin ring. The iron atom is found in the center of the heme and it is coordinated to the four nitrogen atoms of the pyrrol rings. Additionally, the iron can be coordinated to two further binding partners. On the proximal side, this is in peroxidase-peroxygenases usually a cysteine residue and on the distal side, a glutamate. The iron can have two different oxidation states, iron(II) and iron(III). Only in the iron(II) state it is able to bind oxygen (Piontek et al., 2013).

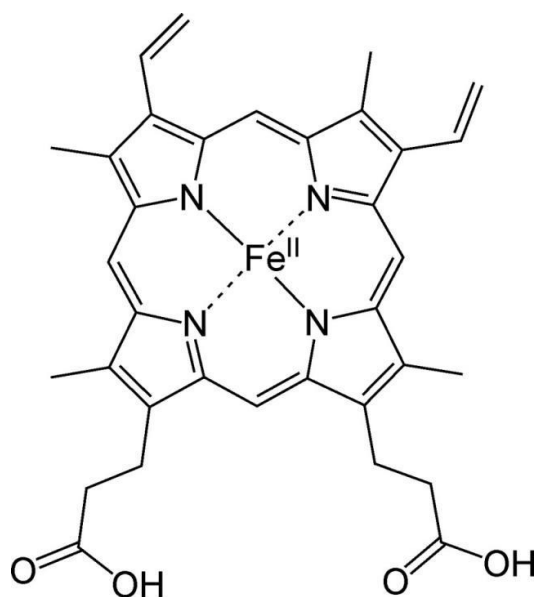


Figure 1-3: Prosthetic group heme *b* with iron(II)

1.2.2 Active site residues in peroxidase-peroxygenases

Sequence alignments show, that in general, peroxidase-peroxygenases possess a highly conserved cysteine-ligand with two bound prolines at the proximal side of the heme. This cysteine-residue significantly distinguishes peroxidase-peroxygenases from other heme peroxidases which have a proximal histidine attached. On the distal side, where the enzymatic activity takes place, on the one hand a conserved glutamic acid residue occurs and on the other hand there is a remarkably variable residue to be found. Furthermore, peroxidase-peroxygenases have a cation-binding site that also shows a highly conserved motif with three ligands: glutamic acid – histidine – aspartic acid (Zámocký *et al.*, 2015).

Figure 1-4 shows the active site of chloroperoxidase. On the proximal side of the heme, there is the characteristic cysteine-residue which is linked to a proline. Both of them a part of a highly conserved motif, namely –X-Proline-Cysteine-Proline-X. On the catalytically active distal side of the heme, a conserved glutamic residue can be found, which is assumed to cleave the O-O bond in hydrogen peroxide during compound I formation (Sundaramoorthy *et al.*, 1995). Additionally, chloroperoxidase have a cation-binding site that shows a highly conserved motif with three ligands: glutamic acid – histidine – aspartic acid (figure 1-4). Also, the serine that coordinates the cation is conserved (Zámocký *et al.*, 2015). However, the cation itself is variable. In case of chloroperoxidase it is a manganese-cation.

Concerning secondary structure, CPO has a 50% helix-content consisting of α - helices and 3_{10} helices. Furthermore, there are two antiparallel β -sheets. There is one disulfide bond and three halide binding sites close to the heme cavity (Kühnel *et al.*, 2006). The distance from the iron to the sulfur of the cysteine ligand is 2.3 Å (Sundaramoorthy *et al.*, 1995).

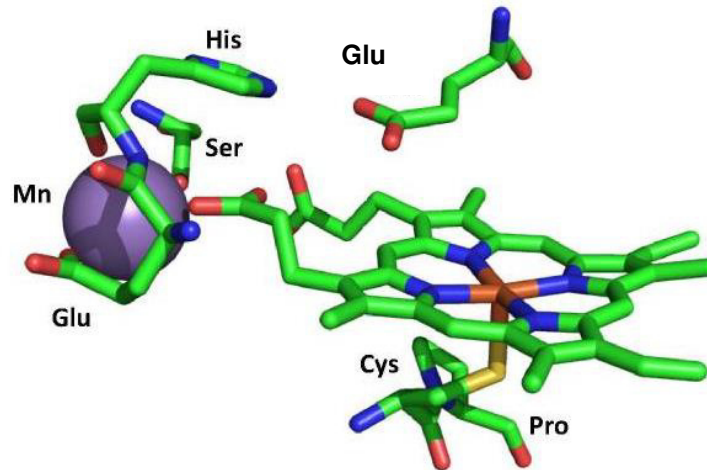


Figure 1-4: Active site structure of chloroperoxidase of *Caldariomyces fumago*,

In figure 1-5 the corresponding active site of unspecific peroxygenase from *Agrocybe aegerita* is displayed. As in CPO there is the proximal cysteine-ligand within the highly conserved –X-P-C-P-X- motif. In UPO, on the distal side of the heme a glutamate and an arginine residue can be found and both residues are involved in compound I formation. The arginine is stabilizing the charges and the glutamate is cleaving the peroxide bond (Piontek *et al.*, 2013). The cation-binding site in UPO includes a magnesium-ion coordinated by a conserved glutamic acid – glycine – aspartic acid (figure 1-5) motif and a serine residue.

The crystal structure of UPO shows a mainly helical secondary structure composition, ten α -helices and five short β -sheets. The heme channel of unspecific peroxygenase is shaped like a cone with its tip cut off and it contains ten aromatic residues, which accompany the substrate into the active center. (Hofrichter *et al.*, 2014) Like chloroperoxidase, UPO shows one disulfide bond and at least one halide binding site in vicinity to the heme cavity. Even the distance from the iron to the sulfur of the cysteine ligand (2.3 Å) is identical to CPO. Super-positioning the structures of both proteins, the active site region shows no major differences (Piontek *et al.*, 2013).

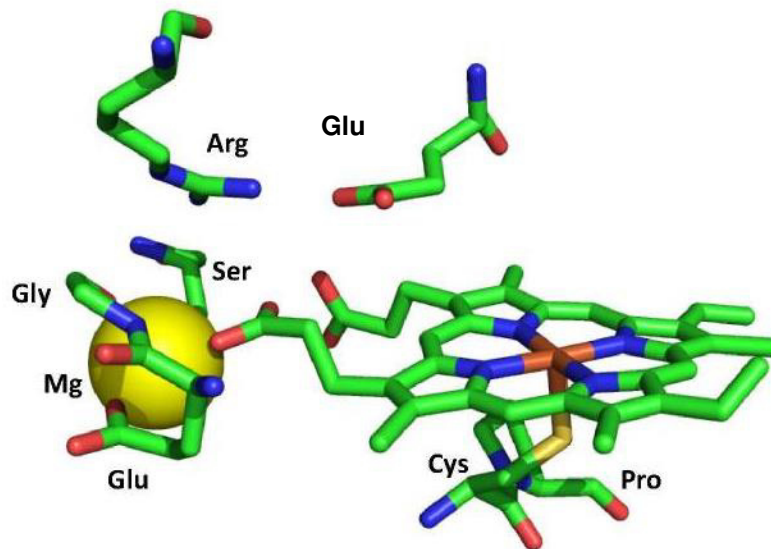


Figure 1-5: Active site structure of unspecific peroxygenase of *Agrocybe aegerita*,

1.3 Reaction mechanism of unspecific peroxygenase

In the first step of the reaction cycle, the substrate *meta*-chloroperoxybenzoic acid is reduced to its corresponding aldehyde, *meta*-chlorobenzaldehyde. Based on the enzyme in the resting state, which means a ferric heme and water bound to the distal side, compound I is formed as depicted in figure 1-6. Compound I formation in UPO is still putative, but it is anticipated, that at first, *m*CPBA binds to the distal side instead of the water molecule. This would result in a transfer of a proton to the glutamic acid residue in close vicinity, followed by forming a so called peroxo-adduct. Secondly, the O-O bond is cleaved heterolytically, generating water and the oxoiron(IV) porphyrin radical cation, which is called compound I (Wang *et al.*, 2012). Afterwards, in an one-electron step, compound I cuts off a proton from the substrate, leading to the ferryl hydroxide complex (figure 1-6), which is compound II, and an alkyl radical. The last step is again a one-electron step that involves the rapidly decaying alkyl radical generating the hydroxylated product of the reaction and the ferric enzyme in the resting state. When the product is discharged, a water molecule binds to the distal side of the heme, allowing the reaction cycle to start again (Wang *et al.*, 2015).

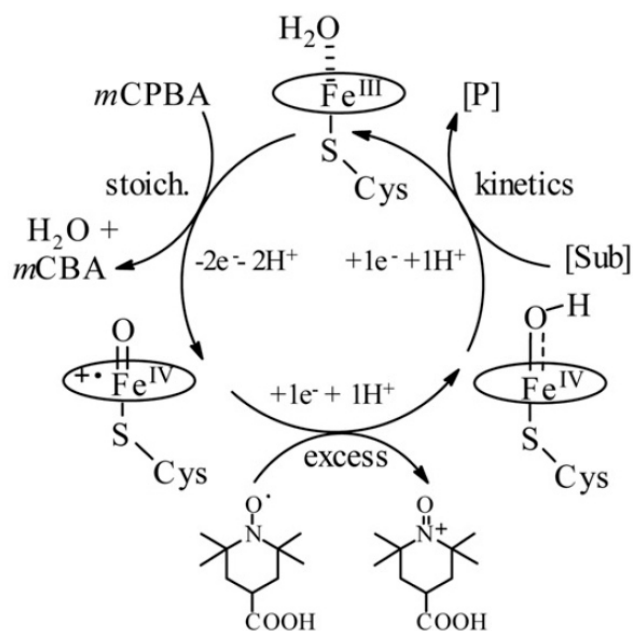


Figure 1-6: Catalytic cycle of unspecific peroxygenase (Wang *et al.*, 2015)

1.4 Industrial applications of peroxidase-peroxygenases

Nowadays, stereoselective enzymatic catalysis of oxygen insertion into organic products (oxyfunctionalization) like alkenes is one of the most desired aims of organic chemistry. But it is a task that is still hardly to achieve. Alkenes are a source for highly requested chemicals like fuels, and they do not have a high occurrence in nature. Therefore they need to be produced synthetically (Bordeaux *et al.*, 2012).

P450 monooxygenases have been in the focus concerning these demands so far, because they are excellent catalysts for oxyfunctionalization reactions. However, they are not stable enough and they need complicated regeneration systems to catalyze oxyfunctionalization (Hofrichter *et al.*, 2014). Reducing equivalents needed by P450 monooxygenase are delivered from NAD(P)H through a mediator system driven by a reductase. The oxidized nicotinamide has to be regenerated afterwards, that is why it is coupled to an enzyme which creates NAD(P)H (figure 1-7 upper).

Here, peroxidase-peroxygenases that are highly interesting for industrial purposes, come into play, because they do not need any of the above

described additional systems. Instead of activating oxygen molecules by reduction, they use hydrogen peroxide for oxyfunctionalization without an intermediate step (figure 1-7 lower).

Besides the less complicated reaction mechanism of peroxidase-peroxygenases, they are remarkable because of their high reaction selectivity, which is usually hard to achieve in combination with high reactivity (Reetz, et al. 2013).

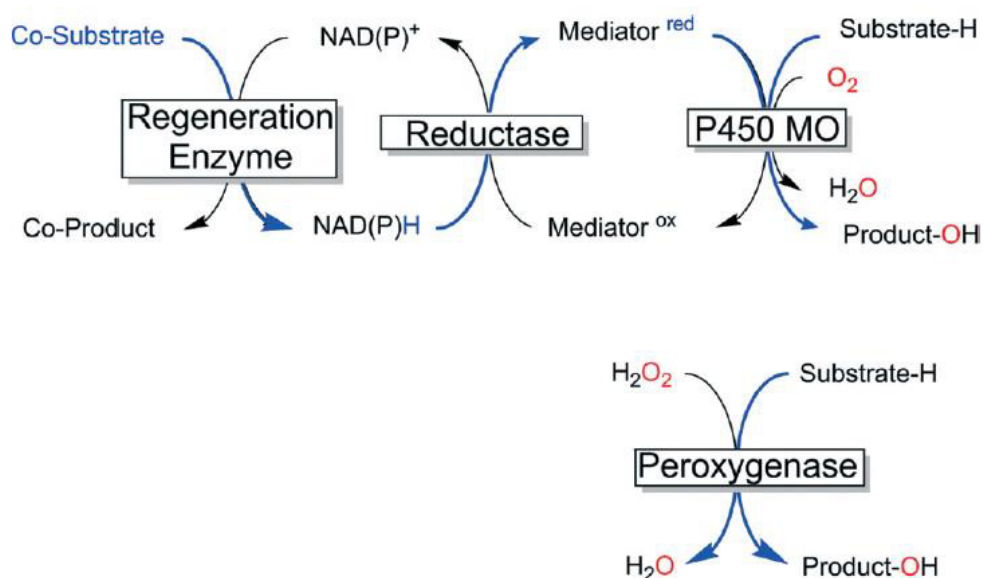


Figure 7: Oxyfunctionalization reaction mechanism for P450-monooxygenase compared to peroxygenases (Bormann et al., 2015)

Not only the complicated structural architecture and the derived complex reaction mechanism of established peroxidase-peroxygenase-predecessors are an issue, but also expression. Heterologous expression of chloroperoxidase could only be achieved in *Aspergillus niger* until today, but with significantly lower yields than in *Caldariomyces fumago*. Compared to that, unspecific peroxygenases, for example from *Agrocybe aegerita* could already be expressed heterologously in *Saccharomyces cerevisiae* and *Pichia pastoris* in relative high yields (Molina-Espeja et al., 2015). This is an important step when it comes to industrial application, although the reaction product yields are still relatively low.

To overcome this problem, genetic engineering has to be applied. There are not many mutants of chloroperoxidase yet, because transformation in *Aspergillus niger* is not very efficient. Unspecific peroxygenase from *Agrocybe aegerita* however, could be mutated successfully with increased enzyme activity and stability (Molina-Espeja *et al.*, 2014).

In summary, the recently discovered peroxidase-peroxygenases are promising enzymes for industrial application because of their ability to catalyze oxyfunctionalization reactions. They show several advantages over their structural relatives chloroperoxidase and P450 monooxygenases as described above. Nevertheless there is still room for improvement, because of their lack of sufficiently high enzyme activity and stability at high temperatures. Additionally, to overcome the self-inhibition by high peroxide concentrations would be a challenge. Also, to increase the number of substrates and the specificity has a big potential for improvement (Bormann *et al.*, 2015).

2 Aim of the thesis

Peroxidase-peroxygenases are a newly classified heme peroxidase subfamily (Zámocký *et al.*, 2015). There are more than one thousand putative homologous peroxidase-peroxygenase sequences available, and almost all of them are to be analyzed if they are functional. (Hofrichter *et al.*, 2014). Besides chloroperoxidase from *Caldariomyces fumago* (CPO) and unspecific peroxygenase from *Agrocybe aegerita* (UPO), very few representatives of this enzyme family have been investigated yet.

As described above, members of this family are very promising for industrial applications, because they are the only enzymes known catalyzing the selective incorporation of oxygen in organic synthesis without an expensive regeneration system. But low expression yields and genetic engineering with regard to inactivation of the peroxygenases at presence of high amounts of hydrogen peroxide, improvable enzymatic activities and stability are tasks that still need to be overcome (Molina-Espeja *et al.*, 2015).

This thesis focuses on the heme-thiolate peroxygenase of *Aspergillus niger* (AnHTP), a peroxidase-peroxygenase related to chloroperoxidase and unspecific peroxygenase from *Agrocybe aegerita*. Using these two excessively researched peroxygenases as model enzymes, AnHTP have to be expressed heterologously, purified and characterized in a similar manner.

AnHTP was expressed heterologously in *Pichia pastoris* in baffled shake flask cultures. *Pichia pastoris* is chosen as expression system because of the relatively high glycosylation degree of heme-thiolate peroxygenases and due to the fact that *Pichia* secretes the target protein, facilitating purification. *Pichia pastoris* is also a standard expression system in bioreactors, which means an uncomplicated upscaling could follow shake flask cultivation. With an attached His₆ tag, an easy one step-chromatography purification protocol was established.

With a wide range of spectroscopic methods, different properties like secondary structure, accessibility of the active center and reducibility were investigated. The size of the enzyme was detected by electrophoresis and size-exclusion HPLC in combination with multi angle light scattering detection.

Additionally, the stability was measured by circular dichroism and differential scanning calorimetry. Moreover, the enzyme activity was determined with steady-state kinetics and the reaction mechanism was solved with stopped-flow spectroscopy.

3 Materials and Methods

3.1 Transformation of *AnHTP* into *Pichia Pastoris* cells

3.1.1 Vector

The vector pJ912 (figure 3-1), purchased from DNA 2.0 contains a methanol inducible alcohol oxidase promoter, a zeocin resistance gene for selecting positive transformed cells, a His₆ tag for affinity chromatography and a gene for the alpha signal sequence. This gene causes the yeast cells to secrete the target enzyme.

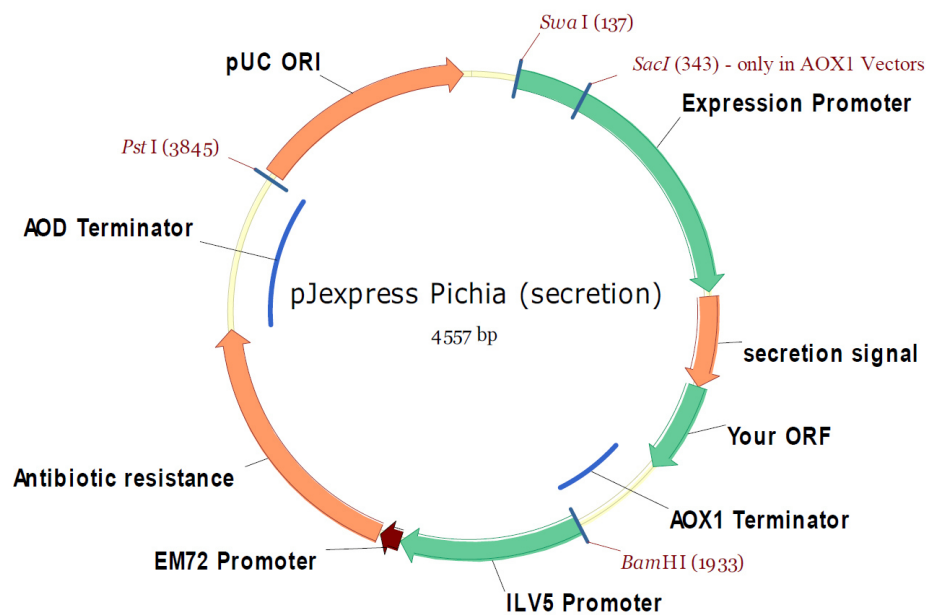


Figure 3-1: Scheme of vector pJ912, figure from DNA 2.0 vector information booklet

3.1.2 Transformation of vector in *E. coli* cells

3.1.2.1 Preparation of heat shock competent cells

In order to perform transformation, *E.coli* cells have to be transferred into a CaCl₂ solution to make the membrane permeable to DNA.

Procedure:

Table 3-1: LB media recipe

LB_(zeo) medium	LB_(zeo) agar
5 g/L yeast extract	5 g/L yeast extract
10 g/L peptone	10 g/L peptone
10 g/L NaCl	10 g/L NaCl
(25 µg/mL zeocin)	15 g/L agar (25 µg/mL zeocin)

7.5 mL Lysogeny Broth (LB) medium was inoculated with a single colony of *E. coli* dH5α cells from an LB agar plate and shaken over night at 180 rpm and 37 °C. Afterwards 100 µL of this culture were added to 50 mL of LB medium. Again the cells were incubated over night at 180 rpm and 37 °C. At an OD₆₀₀ of 0.5 the cells were put on ice for 10 minutes and then centrifuged at 3000 rpm and 4 °C for 10 minutes. The supernatant was discarded and the pellets were dissolved in a precooled CaCl₂ solution. After spinning down the cells for 10 minutes at 3000 rpm and 4 °C again, they were dissolved in a 15 mL precooled solution of CaCl₂ containing glycerol. The cells were aliquoted and frozen at -80 °C.

Material and Equipment

Vector pJ912 with <i>An</i> HTP insert (DNA 2.0)	CaCl ₂ (Sigma)
<i>E.coli</i> dH5α cells	Glycerol (Roth)
Shaking incubator GFL 3033	Yeast extract (Applichem)
Photometer Agilent 8453	Peptone (Applichem)
Centrifuge Sorvall RC-6 with Rotor SS-34	NaCl (Sigma)
Centrifuge Beakers 40 mL	Agar (Roth)
Autoclave 61 GLA 30 (Fritz Gössner Hamburg)	Zeocin (InvivoGen)

3.1.2.1.1 Extraction of DNA

The plasmid DNA was delivered on filter paper, so it had to be extracted.

Procedure:

The filter paper was incubated with sterile dH₂O for 2 minutes. The filtrate was centrifuged at 14000 rpm for 5 minutes. It was measured with a Nanodrop spectrophotometer. The concentration of the plasmid DNA was 31.3 ng/μL.

Material and Equipment

Microcentrifuge Sigma 1-15PK

Photometer Nanodrop 1000 (Peqlab)

3.1.2.2 Transformation

E.coli cells are made chemically competent and heat shocked to perform the transformation. The heat causes the membrane of the bacterial cells to become porous. As a result, the cells take up the plasmid DNA.

Procedure:

The transformation was performed on ice all the time except for the heat-shocking.

50 ng of DNA were added to 50 μL of thawed chemically competent cells. They were incubated for 30 minutes. Furthermore, the cells were heat-shocked at 42 °C for 60 seconds and then put on ice again. 1 mL of SOC medium was added and the cells were incubated again at 180 rpm and 37 °C for one hour. The cells were streaked out on LB_{zeo} agar plates in three different dilutions and incubated over night at 37 °C. A negative control with dH₂O instead of plasmid DNA was also prepared.

A single colony was picked and transferred into an LB_{zeo} medium for further incubation over night at 180 rpm and 37 °C.

Material and Equipment

Heating block Eppendorf thermomixer compact	SOC medium (Agilent)
Incubator (Mettler)	LB _{zeo} medium
Shaking incubator GFL 3033	LB _{zeo} agar

3.1.3 DNA purification

Plasmid DNA binds onto an anion exchange resin, whereas impurities are washed away by a low salt concentration solution. The plasmid DNA can then be eluted by a high salt concentration solution. Afterwards the DNA is concentrated, precipitated with isopropanol and collected by centrifugation.

Procedure:

The plasmid DNA was purified from the *E.coli* cells by using the Quiagen Midi-Prep Kit. The amount of purified DNA was 246.2 ng/μL, measured with the Nanodrop photometer.

The DNA was sent for sequencing in order to check the sequence of the enzyme.

Material and Equipment

Photometer Nanodrop 1000 (Peqlab)
Quiagen Plasmid Midi Kit

3.1.4 Transformation of linearized plasmid DNA in *Pichia* cells

For transformation the *Pichia* strain CBS 7435 was used. This is a Mut^S strain, which means that the cells are not able to metabolize methanol rapidly. The *AOX1* gene is deleted in these strains, thus the biggest part of the alcohol oxidase activity in the cell is lost.

3.1.4.1 Restriction enzyme digestion

In order to take up DNA by *Pichia*, it has to be linearized by a restriction enzyme. This is necessary to activate homologous recombination when the cells are transformed.

Procedure:

Table 3-2: Solutions for restriction enzyme digestion

10x BSA	8 μ L
10x buffer	8 μ L
Plasmid DNA	40 μ L
<i>SacI</i>	4 μ L

10 μ g of plasmid DNA were incubated with 40 ng of *SacI* for 1.5 hours at 37 °C. The DNA was then purified with QIAquick PCR Purification Kit from Qiagen.

Material and Equipment

Bovine Serum Albumin (Sigma)

Heating block Eppendorf thermomixer compact

NeBuffer1 (New England Biolabs)

PCR Purification Kit QIAquick (Quiagen)

SacI 20 U/ μ L (New England Biolabs)

3.1.4.2 Preparation of electrocompetent cells

The cells need to be in a medium of low conductivity to be prepared for electroporation.

Procedure:

Table 3-3: YPD media recipe for electrocompetent cells

YPD _(zeo) medium	YPD _(zeo) agar
10 g/L yeast extract	10 g/L yeast extract
20 g/L peptone	20 g/L peptone
20 g/L glucose	20 g/L glucose
(25 µg/mL zeocin)	10 g/L agar (25 µg/mL zeocin)

30 mL of Yeast Peptone Dextrose (YPD) medium were inoculated with CBS 7435 cells from a cryo culture. The cells were incubated over night at 230 rpm at 28 °C. Afterwards the cells were centrifuged at an OD₆₀₀ of 0.8 with 4000 rpm at 4 °C. The pellet was washed two times with 200 mL of sterile and cooled dH₂O, then dissolved in 200 mL of 1 M sterile and cooled sorbitol. This mixture was again centrifuged with 4000 rpm at 4 °C and the pellet was resuspended in 1 mL of sorbitol. Aliquotes of 80 µL were frozen for storage.

Material and Equipment

Shaking incubator GFL 3033	Sorbitol
Photometer Agilent 8453	Yeast extract (Applichem)
Centrifuge Sorvall RC-6 with Rotor SS-34	Peptone (Applichem)
Centrifuge Beakers 40 mL	Glucose (Sigma)

3.1.4.3 Electroporation

With electroporation the DNA can be inserted into *Pichia* cells. Applying an electrical field makes the yeast membrane highly permeable. Therefore the DNA can be transformed into the cell.

Procedure:

80 µL of electrocompetent cells were mixed with 7 µL of linearized DNA and were incubated for one minute. The mixture was put into a precooled electroporation cuvette which possesses two electrical contacts. Then the electrical field was applied to the cuvette by the electroporator. The device

was set to 2 kV, 200 ohms and 25 μ F. The electroporation was carried out for 4.8 seconds.

The transformed cells were plated on YPD_{zeo} plates and these were incubated for three days at 30 °C.

Material and Equipment

Gene Pulser/Micro Pulser electroporation cuvettes (Bio-Rad)

YPD_{zeo} agar

Micro Pulser electroporator (Bio-Rad)

3.2 Expression screening

An expression screening is the method of cultivating small amounts of single colonies of transformed cells in order to find the genetic clone with the highest activity or another desired comparable parameter. Afterwards this clone is used for further cultivation and expression. Addition of the antibiotic zeocin makes sure that only the cells with zeocin resistance are growing.

Procedure:

10 different single colonies were picked from the YPD_{zeo} plates and 10 mL of BMGY_{zeo} medium per each clone were inoculated under sterile conditions. The cultures were shaken over night at 230 rpm and 30 °C. After 24 hours, protein concentration was measured with the Bradford method and protein activity was determined with an ABTS assay (table 3-5) by the fully automated photometric analyzing device CuBiAn. Additionally the OD₆₀₀ was obtained. According to these three parameters, the best clone was going to be selected.

For the Bradford method, 900 μ L of crude extract were mixed with 100 μ L of Bradford reagent and measured photometrically at 595 nm.

1 mL of the overnight culture was transferred into 9 mL of a new medium, BMMY_{zeo}. The glycerol of BMGY_{zeo} was consumed after 24 hours, so the methanol induction could be started. The cultures were further inoculated at 230 rpm and 25 °C for two more days. Every 24 hours the cultures were

pulsed with 1 mL of 5% (v/v) methanol and the three parameters protein concentration, ABTS activity and OD₆₀₀ and were determined.

4 of the ten clones were growing. On day 3 of the cultivation there were contaminations with bacteria in every culture, which is why the activity values of this day were ignored for the evaluation of the best clone.

Clone 7 was picked for further cultivation because it had the highest specific activity with ABTS.

Table 3-4: ABTS assay for expression screening

ABTS	1 mM
H ₂ O ₂	100 μM
Culture supernatant	undiluted

Table 3-5: Media recipe for expression screening, autoclaved or sterile filtered

YPD _{zeo}	10 g/L yeast extract 20 g/L peptone 20 g/L glucose, autoclaved separately
BMGY _{zeo}	10 g/L yeast extract 20 g/L peptone 100 mL 100 mM potassium phosphate buffer pH 6.0 100 mL 134 g/L yeast nitrogen base with ammonium sulfate without amino acids, filter sterilized 2 mL 0.2 g/L biotin, filter sterilized 100 mL 200 g/L glucose, autoclaved separately
BMMY _{zeo}	10 g/L yeast extract 20 g/L peptone 100 mL 100 mM potassium phosphate buffer pH 6.0 100 mL 134 g/L yeast nitrogen base with ammonium sulfate without amino acids, filter sterilized 2 mL 0.2 g/L biotin, filter sterilized 100 mL 5% methanol

Material and Equipment

Shaking incubator GFL 3033

CuBiAn XC (Optocell technology)

Photometer Agilent 8453

Bradford Reagent (Sigma)

ABTS (Sigma)

H₂O₂ (Sigma)

3.3 Protein production

The recombinant protein was produced in CBS 7435, a *Pichia Pastoris* Mut^S strain. Firstly the cells have to be grown on glycerol to generate biomass. After consumption, methanol must be given for induction of peroxygenase production under the control of the AOX1 promoter. Protein expression was slow because of the strain's lowered alcohol oxidase activity.

With the alpha signal sequence gene, the cells are able to secrete the produced enzyme into the supernatant.

3.3.1 Sterile technique

Working under sterile conditions is crucial for protein expression. It prevents contamination of the cells and protects people working with biological cellular material.

The working steps for protein production were carried out in the laminar flow hood. All of the equipment was disinfected with 70% ethanol before usage. Solutions and part of the equipment like pipet tips were autoclaved. Afterwards biological material and disposable material were decontaminated and discarded. The laminar flow hood was cleaned with 70% ethanol before and after usage. Additionally the UV light was turned on for 30 minutes.

Material and Equipment:

Laminar flow hood Hera safe (Heraeus Instruments)

UV lamp Osram HNS 15 Watt

Ethanol (VWR Chemicals)

3.3.2 Preparation of stock solutions

Hemin was dissolved in 20 mM NaOH, Biotin in hot water and with ultrasound. Both of them were sterile-filtered after dissolution.

The glycerol was diluted 1 to 2 with dH₂O and autoclaved.

As pure methanol is autosterile, it was not autoclaved.

Table 3-6: Concentrations of stock solutions for expression

Hemin	1 mM
Biotin	0.02% (w/v)
Glycerol	50% (v/v)
Methanol	pure

Material and Equipment

Hemin (Sigma)	Syringe 20 mL (Braun)
Glycerol (Roth)	Syringe filter (Roth)
Biotin (Sigma)	Ultrasonic bath Sonorex super RK510H (Bandelin electronic)
Methanol (Sigma)	

3.3.3 Preparation of media and buffers

Media provide the cells with substances they need for growth and protein production.

Peptone is the main protein source, yeast extract also contains amino acids, vitamins and carbohydrates. The additive biotin is an important vitamin and essential for cell growth.

The antibiotic zeocin was added to prevent other microorganisms from growing.

Components like glucose that cannot be autoclaved together with other media components due to the Maillard reaction, were autoclaved separately and added sterilely afterwards.

YP medium

Yeast extract and peptone powder were dissolved in the appropriate amount of dH₂O. This mixture was autoclaved afterwards. To the pre-culture, 1%

glycerol was added and 0.008% biotin was supplemented for further cultivation.

Table 3-7: YP medium recipe

YP medium	10 g/L yeast extract 20 g/L peptone
-----------	--

Buffers

Buffers are important to keep the pH value of a solution at a stable level. At first, the needed salts were weighed in to the amount of the aimed concentration. After that, two third of dH₂O were added to dissolve the salts. The pH value is then set either with HCl or with NaOH, according to whether the desired pH value is acidic or basic. At last, dH₂O was added to the desired final volume.

Below, all used buffer recipe are displayed in the text or in the Material and Equipment-sections.

Material and Equipment

Scale Mettler Toledo PB 300-S/FACT	Glycerol (Roth)
Scale Mettler Toledo AE 240	Biotin (Sigma)
Magnetic stirrer IKAMAG RCT	Zeocin (InvivoGen)
pH meter Radiometer PHM 92	Na ₂ HPO ₄ (Sigma)
Autoclave 61 GLA 30 (Fritz Gössner Hamburg)	NaH ₂ PO ₄ (Sigma)
Peptone (Applichem)	HCl (Roth)
Yeast extract (Applichem)	NaOH (Sigma)

3.3.4 Cultivation of cells

Four Erlenmeyer flasks with 20 mL YP medium with glycerol were inoculated with 330 μ L cryo culture of the verified clone. They were incubated over night at 180 rpm and 28 °C.

Seven 1 L baffled flasks with 200 mL YP-glycerol medium were then supplemented with 0.4 mL of 0.02% (w/v) biotin stock solution and inoculated with 10 mL overnight culture. They were again incubated over night at 180 rpm and 28 °C. After approximately 24 hours the glycerol is completely consumed by the yeast cells. Thus, 2 mL of pure methanol were added to induce protein expression. At this point, also hemin was added to a final concentration of 10 μ M to support heme incorporation. The incubation temperature was lowered to 25 °C for the remaining two days. Methanol was still added every 24 hours.

Material and Equipment

Shaking incubator GFL 3033

Hemin (Sigma)

Pipet aid Pipetus (Hirschmann Laborgeräte)

3.3.5 Harvesting of cells

Four hours after the last methanol addition, the cells were centrifuged at 3000 g and 4 °C for 10 minutes. The pellets were discarded and the supernatant was used for the following ammonium sulfate precipitation.

Material and Equipment

Centrifuge Sorvall RC-6 with Rotor SLA-1500

Centrifuge beaker 400 mL

3.4 Protein purification

As *Pichia* secretes the recombinant protein, cells do not have to be disrupted, the protein is located in the supernatant after centrifugation.

An ammonium sulfate precipitation was carried out because it was discovered that otherwise the His₆ tag is not free for binding to the nickel ions on the chelating sepharose column.

Afterwards the His₆ tagged protein could be purified with metal chelate affinity chromatography and with desalting eventually.

3.4.1 Ammonium sulfate precipitation

Protein precipitation with ammonium sulfate can be a first step for unspecific purification. With a fractionized precipitation at first, media components are removed from the crude extract. Afterwards, other proteins can be eliminated because they differ in their solubility properties from the desired protein. The pellets and the supernatant have to be investigated for containing the target protein after every precipitation step.

Procedure:

The precipitation was performed in two steps. Firstly, 170 g/L of ammonium sulfate powder were added stepwise to the stirred protein solution at 4 °C to achieve a 31% saturation. This procedure was repeated in order to obtain a 62% saturation. The amounts were taken from the ammonium sulfate protein precipitation chart. All steps were carried out on ice or in the cold storage room, so that the protein could not re-dissolve.

Initial concentration of ammonium sulfate	Solid ammonium sulfate (grams) to be added to 1 liter of solution																	
	106	134	164	194	226	258	291	326	361	398	436	476	516	559	603	650	697	
0	79	108	137	166	197	229	262	296	331	368	405	444	484	526	570	615	662	
5	53	81	109	139	169	200	233	266	301	337	374	412	452	493	536	581	627	
10	26	54	82	111	141	172	204	237	271	306	343	381	420	460	503	547	592	
15	0	27	55	83	113	143	175	207	241	276	312	349	387	427	469	512	557	
20		0	27	56	84	115	146	179	211	245	280	317	355	395	436	478	522	
25			0	28	56	86	117	148	181	214	249	285	323	362	402	445	488	
30				0	28	57	87	118	151	184	218	254	291	329	369	410	453	
35					0	29	58	89	120	153	187	222	258	296	335	376	418	
40						0	29	59	90	123	156	190	226	263	302	342	383	
45							0	30	60	92	125	159	194	230	268	308	348	
50								0	30	61	93	127	161	197	235	273	313	
55									0	31	62	95	129	164	201	239	279	
60										0	31	63	97	132	168	205	244	
65											0	32	65	99	134	171	209	
70												0	32	66	101	137	174	
75													0	33	67	103	139	
80														0	34	68	105	
85															0	34	70	
90																0	35	
95																	0	
100																	0	

Adapted from "Data for Biochemical Research" (R.M.C. Dawson, D.C. Elliott, and K.M. Jones, eds.), 2nd Ed. Oxford Univ. Press, London, 1969.

Figure 3-1: Ammonium sulfate precipitation table

The saturated protein solution was centrifuged at 20000 rpm for 45 minutes at 4 °C. The protein was found in the supernatant, this was confirmed by UV/vis spectroscopy and activity measurements with the substrate thioanisole. The supernatant was stored at 4 °C.

Material and Equipment

Centrifuge Sorvall RC-6 with Rotor SS-34

Photometer Hitachi U-3900

Centrifuge beaker 40 mL

Ammonium sulfate (Sigma)

Photometer Agilent 8453

3.4.2 Preparation of the supernatant

A protease inhibitor cocktail was added to the supernatant to prevent proteases from degrading the enzyme. Two tablets per Liter supernatant were dissolved in an ultrasound bath for 15 minutes. The protein solution was then filtered through a 45 µm filter to remove potential column blocking components. The pH value was set to 7.5, otherwise the proteins would not

bind. The supernatant was stored on ice until application on the column was completed.

Material and Equipment

Protease Inhibitor Cocktail Tablets Sigmafast (Sigma)

Ultrasonic bath Sonorex super RK510H (Bandelin electronic)

Vacuum pump CVC2 (vacuumbrand GmbH+Co)

Durapore Membrane filters 0.45 μ M HV (Merck Millipore Ltd.)

pH meter Radiometer PHM 92

3.4.3 Immobilized Metal Ion Affinity chromatography

Histidine-tagged proteins can be easily purified with a chelating column material that is able to bind metal ions, because they have a high affinity to ions like Ni^{2+} .

The immobilized medium consists of iminodiacetic acid groups coupled to a crosslinked form of agarose beads. This is a polymer made of polysaccharides called saccharose.

The column has to be loaded with NiCl_2 to charge the sepharose with metal ions. When the protein solution is applied onto the column, the His_6 -tag of the protein binds to the nickel residues.

For elution, a linear concentration gradient of imidazole is applied. Imidazole has a higher affinity to the nickel ions than histidine, so the desired protein is removed gradually, because the imidazole replaces it at the Ni^{2+} residues.

Procedure:

Table 3-8: Solutions for affinity chromatography

Buffer A	50 mM sodium phosphate buffer 0.5 M NaCl pH 8.0
Buffer B	50 mM sodium phosphate buffer 0.5 M NaCl 0.5 M imidazole pH 7.5
Buffer C	50 mM sodium phosphate buffer 0.5 M NaCl 50 mM EDTA pH 7.5
NiCl ₂	5 g/L

All of the following steps were carried out with a flow rate of 2 mL/min, except for the application of the protein solution. The column was loaded with NiCl₂. Then it was washed with two column volumes of dH₂O to remove excess NiCl₂. Afterwards it was equilibrated applying 3 column volumes of Buffer A. The supernatant was applied to the column overnight. The column was again washed with 4 column volumes of Buffer A to eliminate unbound proteins. The flowthrough was checked with the spectrophotometer to exclude that the target protein doesn't bind. For elution, a gradient former was filled with both Buffer A in one chamber and Buffer B in the other chamber, respectively. Buffer A was stirred to ensure proper mixing after opening the connection between both chambers which leads to starting the concentration gradient. Additionally, a fraction collector was connected to the outlet of the column to collect 2 mL-fractions.

When the connection between the chambers is opened, the two solutions do not mix due to the hydrostatic pressure. Although when the connection of the gradient former to the tube leading to the peristaltic pump is also opened, Buffer A leaves the gradient former and in the same extent, Buffer B enters the

Buffer A-chamber mixing with Buffer A. The amount of Buffer B is increasing with time causing a linear gradient.

Fractions were collected until the UV/vis-Spectrum showed neither a heme peak nor a protein peak. Every fraction was analyzed by the photometer and the fractions containing the desired protein and showed a corresponding spectrum were pooled.

After collecting the fractions, the column needs to be regenerated. Buffer C containing EDTA was applied to the column. EDTA forms a complex with the Nickel ions and so they are removed from the column material. Then remaining unspecific bound components were washed away with 1 M NaOH until the resin looked clean again. The NaOH on the column needs to be neutralized with at least 3 column volumes of dH₂O. Afterwards, the column material was stored in 20% ethanol.

With a centrifugal filter unit called Centriprep, which has a molecular weight cut off at 10 kDa, the pooled fractions were concentrated. The centrifugation increases the hydrostatic pressure of the protein solution on the membrane, causing molecular weight components below 10 kDa and buffer to pass the membrane, whereas bigger molecules like the target protein stay on the other side of the membrane. Thus, the protein solution gets more concentrated. At 4500 g the protein pool was centrifuged for 15 minutes for several times until the sample volume reached a value below 2.5 mL.

Material and Equipment

Column XK 16 (Pharmacia Biotech)	NaH ₂ PO ₄ (Sigma)
Chelating Sepharose Fast Flow (GE Healthcare)	Na ₂ HPO ₄ (Sigma)
Peristaltic Pump P-1 (GE Healthcare)	NaCl (Sigma)
Gradient former Model 385 (Bio-Rad)	NiCl ₂ (Sigma)
Amicon Ultra Centrifugal Filters Ultracel -10K (Merck Millipore)	NaOH (Sigma)
	EDTA (Sigma)
Centrifuge Sorvall RC-6 with Rotor SLA-1500	Imidazole (Sigma)

3.4.4 Desalting

Gel filtration separates molecules according to their size. Small substances diffuse into the column material and are retained from elution longer than bigger molecules which are not able to enter the pores. Because salt molecules are small, they are retained by the porous resin and proteins can be eluted with a buffer that does not contain additional salt.

Especially imidazole has to be removed from the protein solution because it can alter the spectrum and disturb activity measurements.

Procedure:

The PD-10 desalting column was equilibrated with 25 mL of the desired storage buffer for the target protein. In this case a 10 mM sodium phosphate buffer pH 7.0 was used. 2.5 mL of the concentrated protein sample were applied onto the column, the flowthrough was discarded. At last, the protein was eluted with 3.5 mL of the equilibration buffer. The flowthrough was collected and a UV/vis spectrum was obtained to determine the protein concentration and the *Reinheitszahl RZ*. The purified protein solution was stored at 4 °C.

Material and Equipment

Desalting column PD-10 Sephadex G-25M (GE Healthcare)

Photometer Agilent 8453

3.5 Protein characterization

After purifying the protein to the highest purity possible, it can be characterized with a big variety of methods. Its spectral properties, activities and pH-dependency can be analyzed with a photometer. The purity can be determined by SDS-PAGE and western blotting. The stability can be measured with Circular Dichroism and Differential Scanning Calorimetry.

3.5.1 Spectral properties

Peroxidases have characteristic spectral properties. Besides the protein peak, which all proteins show at 280 nm, peroxidases have a so called Soret peak or heme peak. For AnHTP this peak occurs at 423 nm. The purity of the protein solution can be expressed by the ratio between Soret peak and protein peak. The protein concentration can be determined using Lambert Beer's law:

$$A = \epsilon \times c \times d$$

d: cuvette diameter (cm)

A: absorbance

ϵ : molar extinction coefficient ($M^{-1} \text{ cm}^{-1}$)

c: concentration ($\text{mol} \times L^{-1}$)

$$RZ = A_{\text{Soret}}/A_{280}$$

RZ: Reinheitszahl

A_{Soret} : Soret peak absorption

A_{280} : protein peak absorption

3.5.2 Extinction coefficient determination

The extinction coefficient is an important physical quantity to calculate protein concentration as well as parameters that are based on this concentration, like enzyme activities.

Procedure:

The concentration of four different dilutions of the protein, namely 1:5, 1:10, 1:15 and 1:20 was measured by the Bradford method. 1 mL of a 1:5 dilution of the Bradford reagent was mixed with 20 μ L of the respective dilution. Also, a blank with 20 μ L of water instead of protein was prepared. These solutions were incubated for 20 minutes. Afterwards, the absorbance was measured and the concentrations were calculated by the photometer with the already fixed calibration curve. With the same diluted solutions, spectra were obtained to determine the absorbance of the corresponding heme peak.

Material and Equipment

Quartz cuvette 10 mm path length (Hellma Analytics)

Photometer Agilent 8453

Photometer Hitachi U-3900

Bradford reagent (Sigma)

3.5.3 UV/vis spectrum

UV/vis spectra are an easy method to obtain information about the protein solution. Purity, heme incorporation, electron spin states and concentration can be determined this way.

Procedure:

The purified protein solution was diluted with a 10 mM sodium phosphate buffer pH 7.0 to a final volume of 500 μ L. First, a blank was generated with the buffer. Then the spectrum of the enzyme was measured in a range from 250 to 700 nm with a quartz cuvette.

Material and Equipment

Quartz cuvette 10 mm path length (Hellma Analytics)

Photometer Agilent 8453

3.5.4 pH-dependency of the UV/vis spectrum

The pH can have big influence on the spectrum of heme-thiolate peroxygenases. It can alter the characteristic peaks and thus cause a spectral transition.

Procedure:

1 mL of the enzyme solution in a stirred cuvette was titrated to different pH-values ranging from 2.63 to 10.2, controlled by a small pH electrode. Acidic and basic values were obtained with 1 M HCl and 1 M NaOH, respectively. A spectrum was measured for each adjusted pH value.

Material and Equipment

Quartz cuvette 10 mm path length (Hellma Analytics)

HCl (Roth)

Photometer Hitachi U-3900

NaOH (Sigma)

pH electrode FG2 (Mettler Toledo)

3.5.5 Reduction with sodium dithionite

The native form of the iron in the heme *b* of peroxygenases is called ferric. It's the +3 oxidation state of the iron. This state can be reduced to its ferrous form, the +2 oxidation state, by sodium dithionite.

Procedure:

A spectrum of 500 μ L of the protein solution was measured after blanking with the storage buffer (see above). After adding 20 μ L of 100 mM sodium dithionite, another spectrum was recorded.

Material and Equipment

Quartz cuvette 10 mm path length (Hellma Analytics)

Na₂S₂O₄ (Sigma)

Photometer Agilent 8453

3.5.6 SDS-PAGE

Polyacrylamide gel electrophoresis is used to separate biomolecules and to determine their size. Charged macromolecules move in an electrical field according to their charge, size and shape. A marker containing proteins with known molecular weight is used for comparison. Coomassie blue is used to stain the protein.

Procedure:

The two samples were deglycosylated over night at 37 °C before applying on the SDS gel. The components were mixed in the following manner:

Table 3-9: Solutions for deglycosylation

15 µL	AnHTP (1.14 µg/µL)
5 µL	PNGase F buffer
0.5 µL	PNGase F (500.000 U/mL)

One of the samples was reduced with the reducing agent dithiothreitol afterwards.

Table 3-10: SDS-PAGE sample composition

Non-reducing:	15 µL deglycosylated AnHTP solution
	5 µL loading dye
	70 °C, 10 minutes
Reducing:	13 µL deglycosylated AnHTP solution
	5 µL loading dye
	90 °C, 10 minutes

Table 3-11: Loading scheme SDS-PAGE

1	Protein marker
2	AnHTP deglycosylated, non-reduced
3	empty
4	AnHTP deglycosylated, reduced

The gel was running for 80 minutes at 180 V.

It was stained with Coomassie staining solution for 45 minutes and destained in several steps until the background of the gel was clear.

Material and Equipment

XCell Sure Lock™ Electrophoresis Cell (Invitrogen)

Model 1000/500 Power supply (Bio-Rad)

NuPage™ 4-12% Bis-Tris Gel (Invitrogen)

Heating block Eppendorf thermomixer compact

Shaker Ika Vibrax VXR (Janke&Kunkel)

NuPage™ LDS sample buffer (4X) (Invitrogen)

Bolt™ sample reducing agent (10X) (Invitrogen)

peqGOLD Protein-Marker IV (Peqlab)

PNGase F (NEB)

PNGase F buffer pH 8.0:

20 mM Tris-HCl (Sigma)

50 mM NaCl (Sigma)

5 mM EDTA (Sigma)

50% Glycerol (Roth)

Coomassie staining solution:

0.5 g/L Coomassie (Sigma)

20% (v/v) methanol (Sigma)

5% (v/v) acetic acid (Sigma)

25% (v/v) dH₂O

Destaining solution:

40% (v/v) methanol (Sigma)

10% (v/v) acetic acid (Sigma)

50% dH₂O

NuPage™ MOPS SDS Running Buffer (20X) Invitrogen

3.5.7 Western Blot

Western blotting can be used to detect a specific protein in a heterogeneous protein solution. The technique uses antibodies that are specific to a label the protein possesses. After gel electrophoresis the protein with the His₆ tag is transferred to a membrane. The membrane is incubated with a primary antibody specifically binding to the tag. Afterwards a second antibody is added, which binds to the primary antibody as well as it carries an enzyme that

is used for detection. A substrate reacts with the enzyme and generates a coloured product visible as a band.

Procedure:

An SDS gel with the same loading pattern as in table 3-11 was put into the iBlot system of Invitrogen according to the delivered protocol. After 7 minutes the samples were transferred to the nitrocellulosis membrane. It was incubated in blocking buffer and shaken over night at 4 °C. After that, 5 µL of the primary antibody were added, dissolved in 10 mL binding buffer. The membrane was treated with this Penta-His mouse antibody for 2 hours at room temperature, slightly shaking. Then the membrane was washed twice with 10 mL binding buffer to remove excess antibody, before 0.5 µL of the secondary anti-mouse antibody were added. Again incubation for 2 hours at room temperature while shaking. The membrane was now washed four times with binding buffer. Eventually the developing solution was prepared and 5 mL were poured onto the membrane. After 15 minutes incubation time shaking at room temperature, a single band appeared.

Table 3-12: Buffers for Western Blot

<p>Blocking buffer:</p> <p>20 g/L bovine serum albumin (BSA) 20 mL phosphate buffered saline (PBS)</p>	<p>Binding buffer:</p> <p>100 mL PBS 20 µL Tween-20 20 g/L BSA</p>
<p>Developing solution:</p> <p>5 mL alkaline phosphatase buffer (AP) 33 µL nitro-blue tetrazolium (NBT) 16.5 µL 5-bromo-4-chloro-3-indolyl-1-phosphate (BCIP)</p>	
<p>PBS:</p> <p>8.0 g/L NaCl 0.2 g/L KCl 1.81 g/L Na₂HPO₄*2H₂O 0.24 g/L KH₂PO₄ adjust to pH 7.4</p>	<p>AP:</p> <p>12.1 g/L Tris 5.85 g/L NaCl 1.02 g/L MgCl₂ adjust to pH 9.5 with HCl</p>

Material and Equipment

Dry Blotting system iBlot (Invitrogen)	KCl (Sigma)
Shaker Ika Vibrax VXR (Janke&Kunkel)	HCl (Roth)
BSA (Sigma)	Na ₂ HPO ₄ *2H ₂ O (Sigma)
NBT/BCIP (Promega)	KH ₂ PO ₄ (Sigma)
Tween-20 (United States Biochemical)	Tris (Sigma)
NaCl (Sigma)	MgCl ₂ (Sigma)

3.5.8 Steady-state kinetics

Measurement of the catalytic activity of an enzyme provides information about how it works under physiological conditions and about its catalytic mechanism.

With steady-state kinetics the rate-determining step of the reaction mechanism can be illuminated. Information is obtained indirectly by following substrate degradation or product formation. Only a small amount of enzyme is needed for this kind of measurements.

Relating to the Michaelis-Menten kinetics, several significant parameters can be determined:

K_M , the Michaelis constant is a measure for the affinity of the substrate to the enzyme. The lower K_M , the higher the substrate affinity.

k_{cat} is called the turnover number, because it gives the number of substrate molecules that one molecule of enzyme can convert into product in one unit of time.

k_{cat}/K_M , the specificity constant says which substrate the enzyme prefers to catalyze.

Except for the ABTS assay, which generally works best at acidic conditions (pH 5.0), all of the steady-state measurements were carried out under optimal pH-conditions of the enzyme with the respective substrate.

Procedure:

Table 3-13: Assay for pH optimum determinations

Volume	Stock solutions	Final concentration
500 μL	200 mM buffer pH 3.0 to 10	100 mM
100 μL	1 mM to 1 M substrate	100 μM to 100 mM
10 μL	10 mM to 200 mM H_2O_2	100 μM to 2 mM
100 μL	0.77 μM AnHTP	76.9 nM
Rest up to 1 mL	dH_2O	-

The above listed solutions were mixed in a stirred quartz cuvette, the reaction was started with the enzyme and the slope was measured at the detection wavelength for the corresponding substrate formation or degradation for 60 seconds. The pH optimum was determined over a range of pH 3.0 to 10.

3.5.8.1 ABTS assay

Figure 3-2 shows the turnover of ABTS to its corresponding radical cation by peroxidases, respectively peroxygenases.

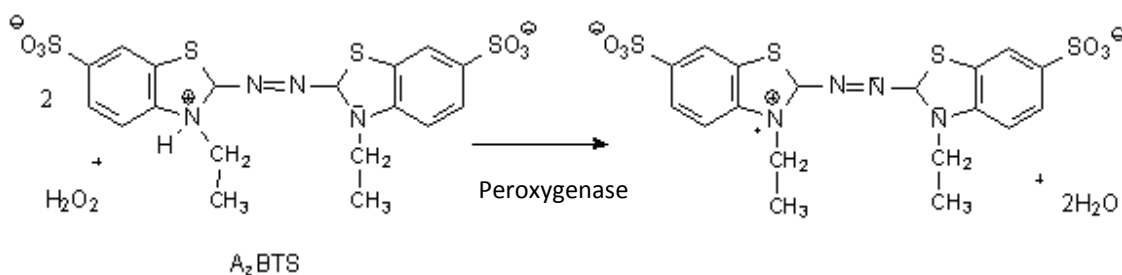


Figure 3-2: Reaction of ABTS to the ABTS radical cation catalyzed by a peroxidase

Peroxidases oxidize ABTS to a green coloured reaction product, the ABTS radical cation. This can be detected with a photometer at 414 nm. The extinction coefficient ϵ of ABTS at 414 nm is $31100 \text{ M}^{-1} \text{ cm}^{-1}$.

Procedure:

Table 3-14: ABTS assay

Volume	Stock solutions	Final concentration
500 μ L	200 mM sodium phosphate buffer pH 5.0	100 mM
5 to 250 μ L	1 mM ABTS	5 to 250 μ M
5 to 30 μ L	10 mM H ₂ O ₂	50, 100, 200, 300 μ M
100 μ L	0.77 μ M AnHTP	76.9 nM
Rest up to 1 mL	dH ₂ O	-

The above listed solutions were mixed in a stirred quartz cuvette, the reaction was started with the enzyme and the slope was measured at 414 nm for 60 seconds. The enzyme activity was measured in U/mg. 1 Unit is defined as the amount of enzyme that oxidizes 1 μ mol of ABTS per minute at pH 5.0 and 25 °C.

Material and Equipment

Quartz cuvette 10 mm path length (Hellma Analytics)

ABTS (Sigma)

Photometer Hitachi U-3900

30% (w/w) H₂O₂ (Sigma)

3.5.8.2 Catalase activity

Catalase activity can be measured with a Clark-type electrode. It measures oxygen tension amperometrically. A silver anode and a platinum cathode are immersed in an electrolyte solution which consists of buffer, hydrogen peroxide and water. The oxygen generated by the reaction of the injected enzyme with hydrogen peroxide reaches the cathode by passing through a permeable Teflon membrane. There the oxygen is reduced. Because of the reduction, a current flows and the resulting potential difference is recorded.

Procedure:

Table 3-15: Catalase activity assay

Volume	Stock solutions	Final concentration
1000 μ L	200 mM sodium phosphate buffer pH 5.0	100 mM
75 to 200 μ L	40, 100, 200 mM H ₂ O ₂	1 to 40 mM
20 μ L	4.9 μ M AnHTP	49 nM
Rest up to 2 mL	dH ₂ O	-

The reaction chamber is connected to a water bath to maintain a constant temperature of 30 °C. This is required, because oxygen solubility in water is temperature dependent. The assay components need to be stirred constantly during the measurement. Buffer, H₂O₂ and dH₂O were put into the reaction chamber first. Before the actual measurement, the electrode needed to be calibrated in a two-point procedure. First, the oxygen concentration in the air flushed water-buffer mixture was measured and when it reached a constant level, it was set as the first point. By introducing gaseous nitrogen, the oxygen in the solution was removed to calibrate the electrode to zero. Subsequently, for the actual measurement, nitrogen was introduced again to completely remove the oxygen from the solution. Then, after covering the reaction cell with a lid, the enzyme solution was injected into the chamber and the oxygen rate increase was measured at different H₂O₂ concentrations.

Material and Equipment

Clark-type electrode Oxygraph 11125 (Hansatech)	50 μ L syringe (Hamilton)
Thermostat Medingen E5	30% (w/w) H ₂ O ₂ (Sigma)

3.5.8.3 Thioanisole Assay

Peroxygenases can react very specifically with thioanisole, thereby oxidating the sulfur atom in the compound (figure 3-3).

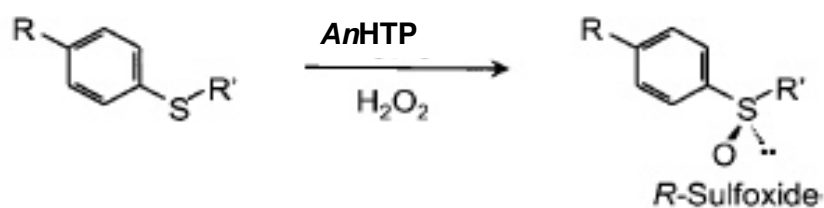


Figure 3-3: Reaction of thioanisole to its corresponding sulfoxide catalyzed by *AnHTP*

Thioanisole is oxidized to the corresponding sulfoxide. The reaction product of the sulfoxidation caused by *AnHTP* can be monitored at 250 nm. The extinction coefficient ϵ of thioanisole at this wavelength is $9700 \text{ M}^{-1} \text{ cm}^{-1}$.

Table 3-16: Thioanisole assay

Volume	Stock solutions	Final concentration
500 μL	200 mM Sodium phosphate buffer pH 5.0	100 mM
5 to 100 μL	1 mM Thioanisol	5 to 100 μM
10 μL	100 mM H_2O_2	1 mM
100 μL	0.77 μM <i>AnHTP</i>	76.9 nM
Rest up to 1 mL	d H_2O	-

The above listed solutions were mixed in a stirred quartz cuvette, the reaction was started with the enzyme and the decrease of absorbance was measured at 250 nm for 60 seconds. The enzyme activity was measured in U/mg. 1 Unit is defined as the amount of enzyme that oxidizes 1 μmol of thioanisole per minute at pH 5.0 and 25 $^\circ\text{C}$.

Material and Equipment

Quartz cuvette 10 mm path length (Hellma Analytics)

Thioanisol (Sigma)

Photometer Hitachi U-3900

30% (w/w) H_2O_2 (Sigma)

3.5.8.4 Veratryl- and vanillyl alcohol assay

Figure 3-4 shows the oxidation of veratryl alcohol to its corresponding aldehyde and acid by a peroxygenase.

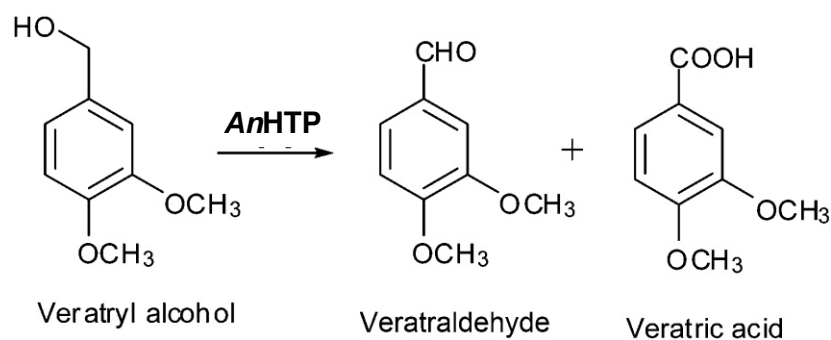


Figure 3-4: Reaction of veratryl alcohol to its products veratraldehyde and veratric acid catalyzed by AnHTP

Heme-thiolate peroxygenases convert alcohols into their corresponding aldehydes and their acids. For veratryl alcohol, the extinction coefficient ϵ is $9300 \text{ M}^{-1} \text{ cm}^{-1}$ at 310 nm and the formation of its aldehyde was measured at this wavelength. For vanillyl alcohol the extinction coefficient is $4400 \text{ M}^{-1} \text{ cm}^{-1}$ at 287 nm and the formation of vanillic acid was measured at this wavelength.

Table 3-17: Veratryl alcohol assay

Volume	Stock solutions	Final concentration
500 μL	200 mM sodium phosphate buffer pH 7.0	100 mM
5 to 100 μL	100 mM veratryl alcohol	500 μM to 10 mM
20 μL	100 mM H_2O_2	2 mM
100 μL	0.77 μM AnHTP	76.9 nM
Rest up to 1 mL	dH ₂ O	-

Table 3-18: Vanillyl alcohol assay

Volume	Stock solutions	Final concentration
500 µL	200 mM sodium phosphate buffer pH 7.0	100 mM
5 to 100 µL	1 mM vanillyl alcohol	5 µM to 100 µM
10 µL	10 mM H ₂ O ₂	100 µM
100 µL	0.77 µM AnHTP	76.9 nM
Rest up to 1 mL	dH ₂ O	-

The above listed solutions were mixed in a stirred quartz cuvette, the reaction was started with the enzyme the increase of absorbance was measured at 310 nm for veratryl alcohol and at 287 nm for vanillyl alcohol for 60 seconds. The enzyme activity was measured in U/mg. 1 Unit is defined as the amount of enzyme that oxidizes 1 µmol of veratryl or vanillyl alcohol per minute at pH 7.0 and 25 °C.

Material and Equipment

Quartz cuvette 10 mm path length (Hellma Analytics)

Vanillyl alcohol (Sigma)

Photometer Hitachi U-3900

30% (w/w) H₂O₂ (Sigma)

Veratryl alcohol (Sigma)

3.5.8.5 Taurine-Bromide assay

With the β- amino acid taurine as a substrate, peroxygenases are able to oxidize halides into their corresponding hypohalous acids, using hydrogen peroxide as cosubstrate.



Figure 3-5: Reaction of bromide with hydrogen peroxide to hypobromous acid catalyzed by AnHTP

In this case, the used halide was bromide which is converted into hypobromous acid by AnHTP. Afterwards, the substrate taurine reacts with

hypobromous acid, forming taurine bromamide (Weiss *et al.*, 1982). The increase of this product can be measured at 289 nm. The extinction coefficient for taurine bromamide is $415 \text{ M}^{-1} \text{ cm}^{-1}$ at this wavelength.

Table 3-19: Taurine-Bromide assay

Volume	Stock solutions	Final concentration
500 μL	200 mM sodium phosphate buffer pH 7.0	100 mM
5 to 100 μL	100 mM taurine	500 μM to 10 mM
100 μL	1 M potassium bromide	100 mM
10 μL	10 mM H_2O_2	100 μM
100 μL	0.77 μM AnHTP	76.9 nM
Rest up to 1 mL	d H_2O	-

The above listed solutions were mixed in a stirred quartz cuvette, the reaction was started with the enzyme the increase of absorbance was measured at 289 nm for 60 seconds. The enzyme activity was measured in U/mg. 1 Unit is defined as the amount of enzyme that oxidizes 1 μmol of taurine per minute at pH 7.0 and 25 °C.

Material and Equipment

Quartz cuvette 10 mm path length (Hellma Analytics)	Potassium bromide (Merck)
Photometer Hitachi U-3900	30% (w/w) H_2O_2 (Sigma)
Taurine (Sigma)	

3.5.9 Sodium cyanide titration

Cyanide can act as an inhibitor with peroxygenases. It binds tightly to the iron(III) of the heme, which results in the conversion of the high-spin to a low-spin electron state. This process alters the absorption of the heme peak. So it can be detected photometrically.

Procedure:

500 μL of a 3.8 μM enzyme solution in a 10 mM sodium phosphate buffer pH 7.0 were titrated in a quartz cuvette with sodium cyanide until a spectral alteration was observed.

After every addition of a cyanide portion a UV/vis spectrum was measured from 250 to 700 nm. Because the final concentration changes with added volumes of cyanide, a correction of the concentration was necessary. The change of absorption at 424 nm was determined and plotted against the corrected cyanide concentrations.

Material and Equipment

Quartz cuvette 10 mm path length (Hellma Analytics)

Sodium cyanide (Sigma)

Photometer Agilent 8453

3.5.10 Circular dichroism

Proteins, amongst other chiral molecules, absorb left circularly polarized light to a different extent than right circularly polarized light. This difference is called ellipticity and it is measured over a wavelength range to determine the secondary structure of a protein. But it can also be used to measure the dichroism at one wavelength over a temperature range to obtain information about the thermal stability of a protein.

Procedure:

At first, a blank needed to be measured with the same parameters applied for the spectra afterwards. The storage buffer of the enzyme, a 10 mM sodium phosphate buffer pH 7.0 was used. Subsequently, the 300 μL cuvette was filled with a 3.8 μM enzyme solution and a spectrum in the far-UV region from 180 to 260 nm was obtained at 20 °C. Then, at 222 nm the dichroism was measured over a temperature range from 20°C to 90 °C. Finally, another spectrum in the far-UV region was obtained to observe structural changes caused by heating. The same procedure was carried out for the near-UV and visible region from 250 to 500 nm, except that a larger amount of enzyme

solution of 3 mL was needed. The temperature curve in the visible range was recorded at 431 nm. The spectral bandwidth for the far-UV region was set to 3 nm and the bandwidth for the visible region was set to 1 nm. The scan speed was 10 s nm⁻¹ for spectra and temperature curves. The pathlength for the far-UV measurements was 1 mm and 10 mm for the measurements in the visible range.

Secondary structure composition was calculated with the program CDNN, a protein secondary structure analysis tool. For the calculation, following parameters were used: number of amino acids (*An*HTP consists of 342 amino acids), the signal was measured in millidegrees, the protein concentration was 3.8 μM and the cuvette thickness was 1 mm.

Material and Equipment

Spectropolarimeter Chirascan (Applied Photophysics)

QS High Precision Cell, Light Path 1 mm (Hellma Analytics)

QS High Precision Cell, Light Path 10 mm (Hellma Analytics)

3.5.11 Differential scanning calorimetry

A Differential scanning calorimeter (DSC) measures the difference in heat energy uptake of a sample in comparison to a reference solution. When a protein solution is heated at the same time as its buffer reference, the difference in the amount of energy that is needed to keep both solutions at the same temperature is measured. In this case, the method was used to gain information about the thermal stability of the enzyme and thus compare the results with the CD-measurements.

Procedure:

500 μL of a 7.2 μM *An*HTP solution were pipetted into the well plate next to two wells filled with 500 μL of storage buffer (10 mM sodium phosphate buffer pH 7.0). There was a buffer run before the sample was measured and three washing runs with dH₂O after the sample run. The settings of the DSC device

comprised a temperature increase from 20 °C to 100 °C with a rate of 1 °C per minute at 4.136 bar cell pressure.

Material and Equipment

Differential scanning calorimeter VP Capillary DSC with Autosampler (Microcal)

Sample plates VP-CAP DSC, WEL 190010-010, 500 µL (Microcal)

3.5.12 Size-exclusion HPLC

Size-exclusion chromatography is a molecule separation technique. Molecules with a small size are more likely to enter the porous column material in contrast to bigger molecules. So the interaction of the smaller molecules with the resin is stronger than the interaction with bigger molecules. They are therefore eluted first and have a shorter retention time. The eluted molecules then pass a detector, in this case a multi-angle light scattering detector. Collimated light from a laser source is directed to the sample and because of the way how the sample scatters light, the molar mass of the molecule can be determined.

Procedure:

To determine the molar mass and to find out whether the enzyme occurs as a monomer or a dimer, size-exclusion chromatography together with multi-angle light scattering was performed. The pore size of the column material is 13 µm. The column was equilibrated with a PBS buffer with 200 mM NaCl and afterwards 37 mL, which equals 38 µg, of the undiluted enzyme were injected. The flow rate was 0.75 mL per minute.

Material and Equipment

HPLC Shimadzu prominence LC20

Column Superdex 200 10/300 GL (GE healthcare)

MALS detector WYATT Heleos Dawn8+ plus QELS,
software ASTRA 6

Diode array detector SPD-M20A
(Shimadzu)

Dulbecco's PBS buffer with 200 mM NaCl
(Sigma)

3.5.13 Stopped-flow spectroscopy

Stopped-flow spectroscopy is a method used for investigating fast reactions in a time scale of milliseconds. Thereby, two reactants are rapidly mixed together by pushing them through a mixer with a mechanical drive as shown in figure 3-6 and then into the observation cell. This process pushes the leftover solutions of the cell into the stop syringe. Then the piston triggers the switch and data collection starts. Monochromatic light irradiates the sample in the observation cell and the change of the signal caused by the reaction of the two solutions is recorded. The signal can be a fluorescence signal or the absorbance at a specific wavelength. The signal is recorded as a function of time. The resulting data can be used for the determination of reaction rates, reaction intermediates and reaction mechanisms.

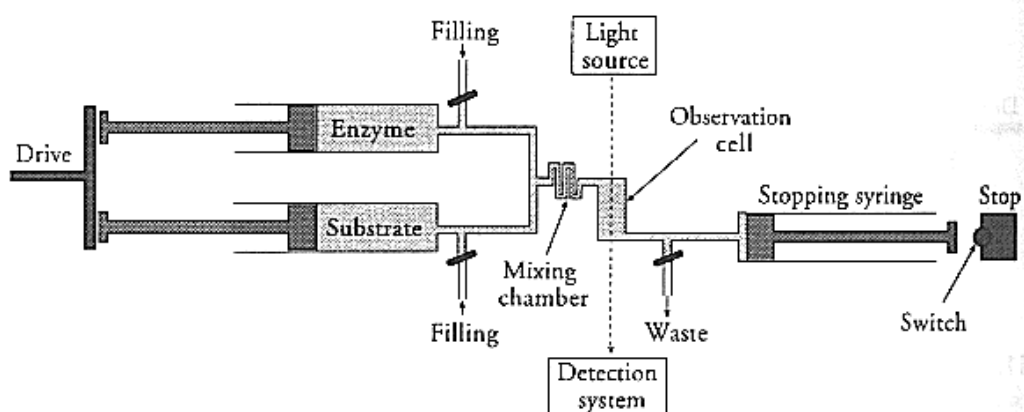


Figure 3-6: Scheme of stopped-flow apparatus with conventional mixing mode

The time right after mixing is called pre-steady-state. It is the very short time span before an equilibrium is achieved. Thereby, the dead time of the stopped-flow device has to be taken into consideration. It is the time between mixing and the start of the observation of the reaction and is usually about 1 millisecond. During that time, no measurements can be done, because the reactants are not in the observation cell yet.

The stopped-flow device can be used in two modes, the conventional mixing mode and the sequential mixing mode. In the first one, two reactants can be

mixed, whereas in the second one up to four reactants can be applied. The photodiode array detector is used to measure spectra and the photo multiplier is used for measuring at single wavelengths.

Procedure:

Photodiode array measurements were conducted using the conventional mixing mode. Absorbance spectra were determined in a wavelength range of 250 to 750 nm within a time of 10 seconds. 2000 data points were obtained in a logarithmic scale at 425 nm wavelength.

The enzyme, in a 10 mM sodium phosphate buffer pH 7.0, as well as the substrate solutions, were mixed in equal volumes. The enzyme concentration was 2.4 μM , whereas the substrate concentrations were varied (25, 30, 40, 50, 60 and 70 μM). *meta*-chloroperoxybenzoic acid was used as substrate. Before starting the measurements, a dH₂O blank needed to be conducted. The drive syringes were filled with both reactants and the reaction was started with the software. Afterwards the system needed to be washed with dH₂O several times.

Material and Equipment

Stopped-flow spectrometer SX.18MV-R (Applied Photophysics)

2 mL disposable syringes (Braun)

meta-chloroperoxybenzoic acid (Fluka)

4 Results and Discussion

4.1 Expression screening

To find the genetic clone with the highest activity and thus to produce the highest possible amount of active enzyme, an expression screening was performed.

Four clones out of ten were growing, the one with the highest activity was picked for further cultivation. The enzyme activity could be measured directly in the supernatant, because the enzyme was secreted from the cell. The activity values at 72 hours were excluded due to contamination.

The concentration of the protein in (mg/mL) was obtained by the Bradford method, the ABTS activity in (U/mL) was measured.

Specific activity (U/mg) = activity (U/mL) / concentration (mg/mL)

1 Unit is defined as the amount of enzyme that oxidizes 1 μmol of ABTS per minute at pH 7.0 and 25 °C.

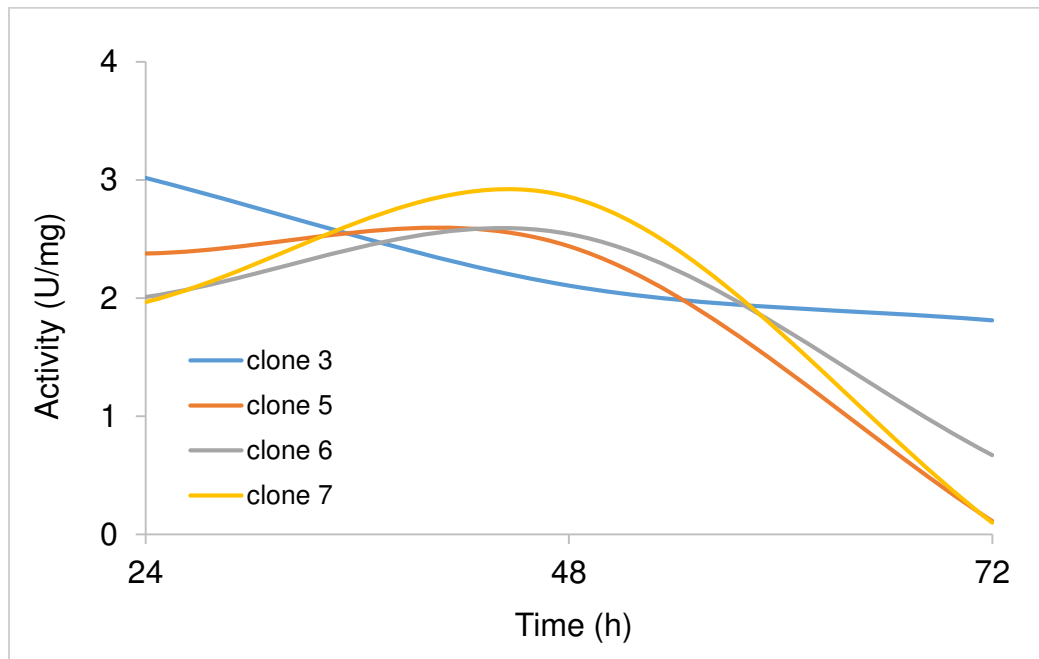


Figure 4-1: Specific activity progress of screened clones over 72 hours

Clone 7 had the highest specific activity at 48 hours, so it was selected for further cultivation.

4.2 Protein purification

The purification procedure of the enzyme is quite straightforward. Only four steps lead to the purified enzyme. The supernatant, gained by centrifugation, was precipitated with ammonium sulfate, purified with metal chelate affinity chromatography, concentrated afterwards and finally desalted by changing the buffer into a 10 mM sodium phosphate buffer pH 7.0. After each of these steps, a UV/vis spectrum was obtained (figure 4-2). There are only small changes in the spectrum during the purification procedures. The *Reinheitszahl* ($RZ = A_{\text{Soret}}/A_{280}$) after affinity chromatography is 0.97 and it changes to 1.2 after concentrating the sample, whereas the Soret peak remains at 424 nm.

Chapter 4.4 goes more into detail on the UV/vis spectrum of the peroxygenase.

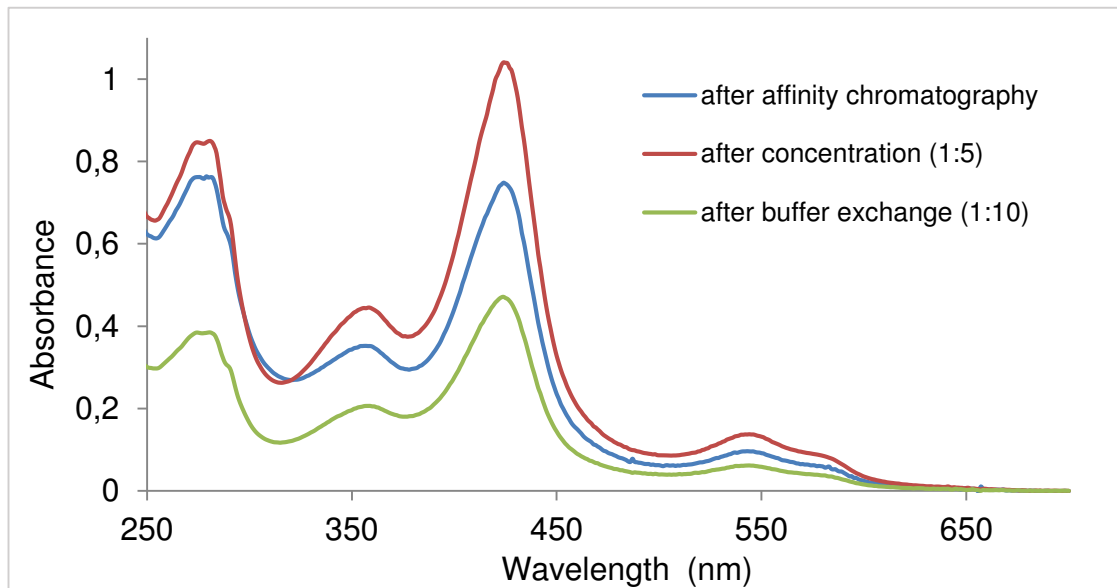


Figure 4-2: UV/vis spectra of AnHTP during purification process

Figure 4-3 shows an SDS-PAGE, which displays the differences between the glycosylated and deglycosylated enzyme, as well as the influence of a reducing agent on this protein. The same figure also shows a Western blot. The SDS-gel was stained with Coomassie Blue and the Western blot was detected with an anti-His antibody.

In lane 1, the purified non-reduced glycosylated protein was applied. It shows a long smear between 55 and 70 kDa. This indicates a rather highly glycosylated protein. Lane 2 displays the same result, however the sample was reduced. Reduction obviously does not change the appearance of the glycosylated enzyme. In lane 3 and 4, the protein was deglycosylated, in lane 4 it was additionally reduced. The theoretical size of the heme-thiolate peroxxygenase is 28345 Da. That is where the bands in lanes three and four appeared. In lane three there is an additional band at approximately 60 kDa, which might be the remaining glycosylated protein. The various small fragments in lane three and four between 5 and 15 kDa are probably degradation products of the deglycosylation with the enzyme PNGase F. Particularly because these bands do not show in the lanes with the glycosylated protein.

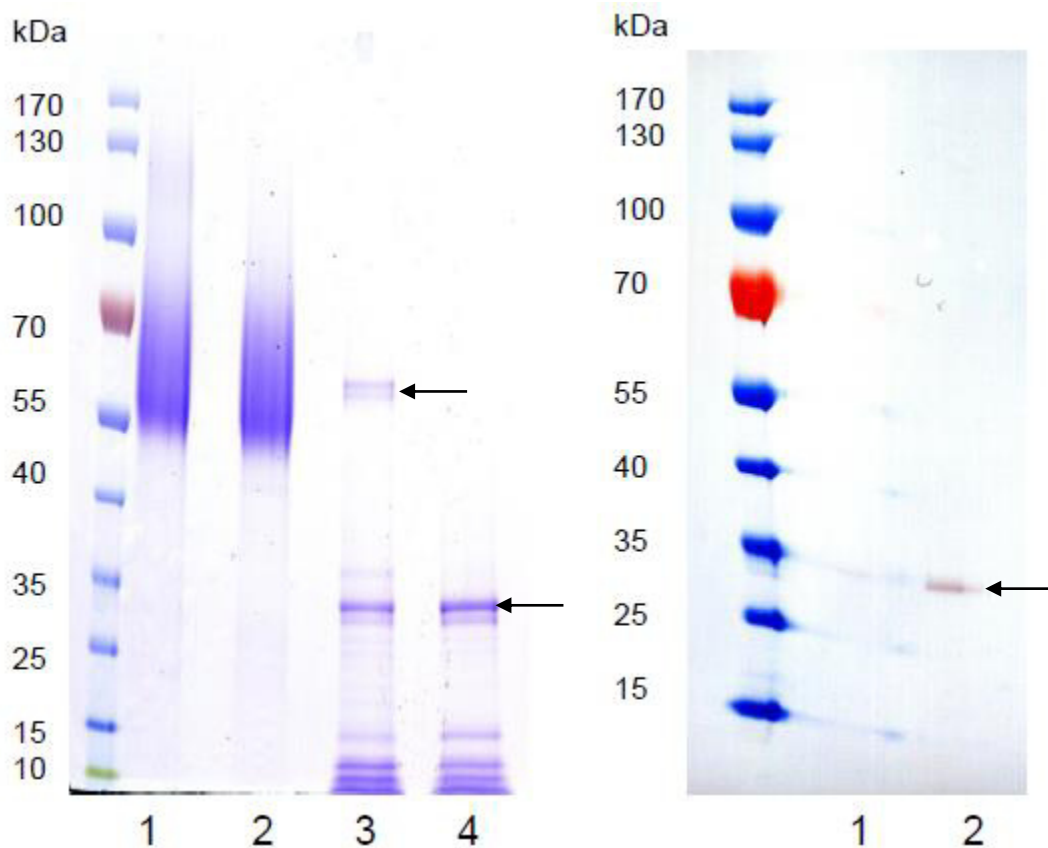


Figure 4-3: SDS-PAGE of non-reduced (lane 1 and 3) and reduced (lane 2 and 4), glycosylated (lane 1 and 2) and deglycosylated (lane 3 and 4) *AnHTP* and Western Blot of deglycosylated *AnHTP*, non-reduced (lane 1) and reduced (lane 2)

Lane 1 and 2 of the Western blot show the non-reduced and reduced deglycosylated samples. With the reduced sample, a band at approximately 28 kDa appeared, which corresponds to the theoretical size of the protein. With the non-reduced sample, only a very weak band appeared at this height.

From the SDS-gel, an approximate glycosylation degree can be calculated: If the deglycosylated protein is about 28 kDa and the average size of the glycosylated protein is $(55 \text{ kDa} + 70 \text{ kDa})/2 = 62.5 \text{ kDa}$ (because of the heterogeneous glycosylation an average value has to be used for calculation), the glycosylation degree is roughly 45%.

Generally, from the SDS-PAGE it can be concluded that the protein is pure and highly glycosylated.

Estimated from amino acid composition, the unspecific peroxygenase from *Agrocybe aegerita* has a molecular weight of 51.1 kDa (Molina-Espeja *et al.*, 2014), whereas the heme-thiolate peroxygenase of *Aspergillus niger* has a theoretical molecular weight of 28.3 kDa. Even if the *An*HTP is smaller, the glycosylation degree of approximately 45% is higher compared to 30% of UPO (Molina-Espeja *et al.*, 2014). Additionally, the glycosylation of UPO does not vary over such a big range than it does with *An*HTP. UPO has 6 predicted glycosylation sites, whereas *An*HTP has 9 predicted glycosylation sites (Molina-Espeja *et al.*, 2014). Assuming that an increasing degree of glycosylation and number of glycosylation sites complicates the glycosylation process in the cell, the higher degree of heterogeneity in glycosylation of *An*HTP compared to UPO could be explained.

4.3 Extinction coefficient determination

The extinction coefficient was determined to calculate the protein concentration based on UV/vis spectra and for determination of the kinetic constants. The concentrations in (mol/L) of different protein dilutions were determined with the Bradford method and then plotted against the Soret-maxima at 424 nm. From the slope of the generated linear fit (figure 4-3), the extinction coefficient of the enzyme, which is $129996 \text{ M}^{-1} \text{ cm}^{-1}$, can be deduced.

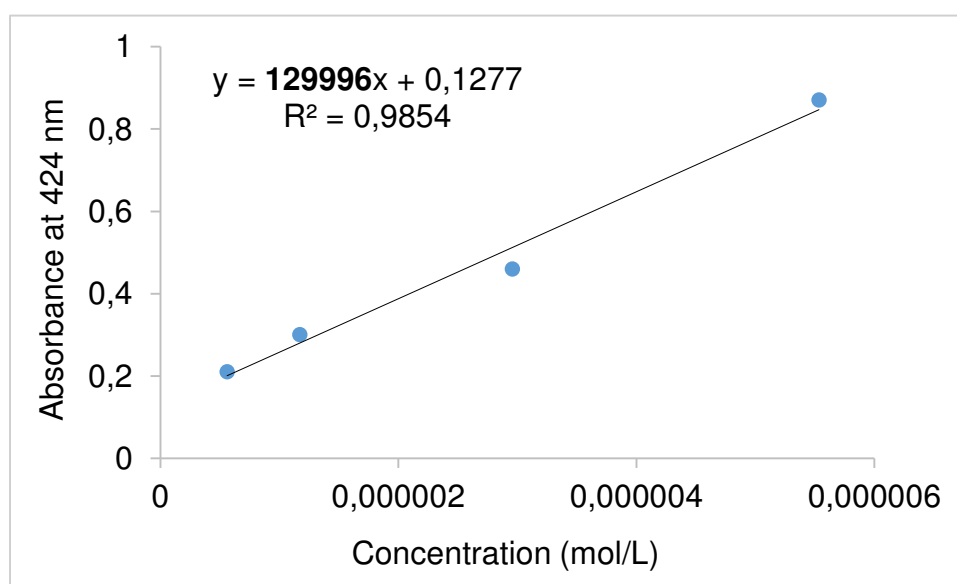


Figure 4-4: Soret maxima at different *AnHTP* concentrations

4.4 UV/vis spectrum

A UV/vis spectrum is one of the most characteristic features of heme peroxygenases. Various different information can be obtained by analyzing it. Purity, electronic configuration, heme incorporation and concentration can be determined.

Because the enzyme showed to be stable in a 10 mM sodium phosphate buffer pH 7.0, all UV/vis spectra were determined in this buffer solution.

The *AnHTP* typical Soret-peak appears at 424 nm, see figure 4-4. The ratio between the absorbance of the Soret-peak and the absorbance of the general protein peak at 280 nm is 1.2 and is called *Reinheitszahl RZ*. It is a measure for purity and heme occupancy. The absorbance at 280 nm is due to the absorbance of the aromatic amino acids. The protein peak shows no additional shoulder, which indicates that there is no DNA or RNA impurities in the protein solution. The spectrum of *AnHTP* shows a for heme-thiolate peroxygenases characteristic δ band (Hager *et al.*, 1986) at 359 nm and two so called Q_{α} and Q_{β} bands at 579 nm and 544 nm. They suggest the electron configuration of the iron in the center of the heme. Together with the blue-

shifted Soret-peak, the Q bands indicate a low-spin state of the heme iron in this spectrum.

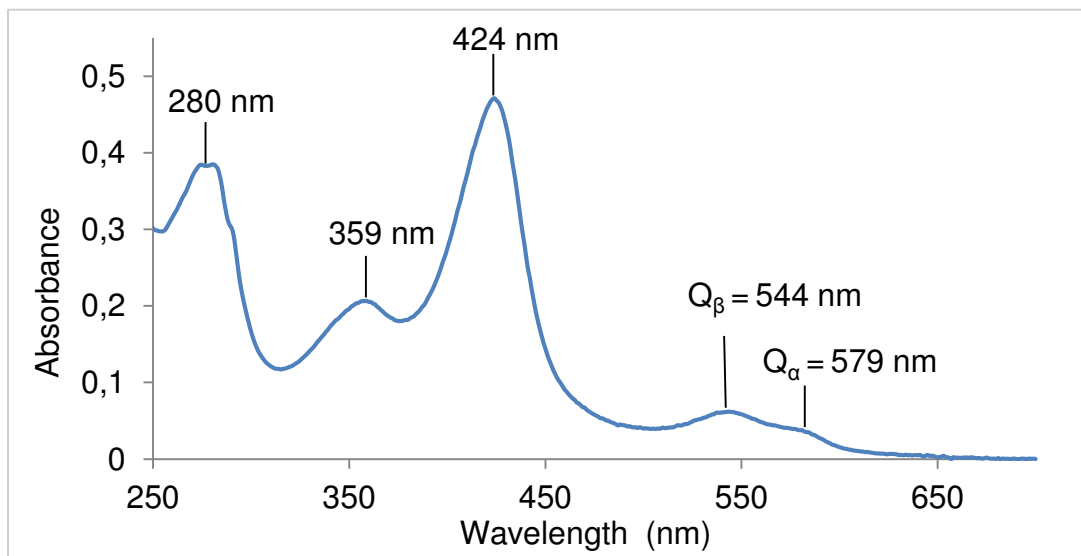


Figure 4-5: UV/vis spectrum of purified *AnHTP*

Comparing the *RZ* value for UPO and *AnHTP*, the *RZ* value for UPO is twice as high as the value for *AnHTP*. On the basis of high protein purity with both enzymes proven by SDS-PAGE, the reason for the different *RZ* values might be the different in molecular mass. For UPO it is approximately 46 kDa (Molina-Espeja *et al.*, 2014), for *AnHTP* it is 28 kDa. Maybe it is possible to achieve a higher purity for *AnHTP* with size exclusion chromatography, especially in its deglycosylated form, but that remains to be elucidated. The Soret peak of both peroxygenases is quite similar and also the Q bands are comparable (Molina-Espeja *et al.*, 2014).

Except for the *Reinheitszahl*, the spectroscopic features of both enzymes are almost identical which could be a hint for similar catalytic behavior and similar active site structure.

Table 4-1: Spectroscopic features of *An*HTP and UPO

Spectroscopic feature	<i>An</i> HTP	UPO
$RZ (A_{\text{Soret}}/A_{280})$	1.2	2.4
Soret peak (nm)	424	420
Q_{α} (nm)	579	572
Q_{β} (nm)	544	540

4.5 Size exclusion HPLC

The size exclusion HPLC was carried out to elucidate and confirm the molecular weight, the purity and the oligomeric state of *An*HTP. Because the highly glycosylated protein which showed a smear on the SDS-PAGE about twice the theoretical size, the question whether it forms a dimer arose.

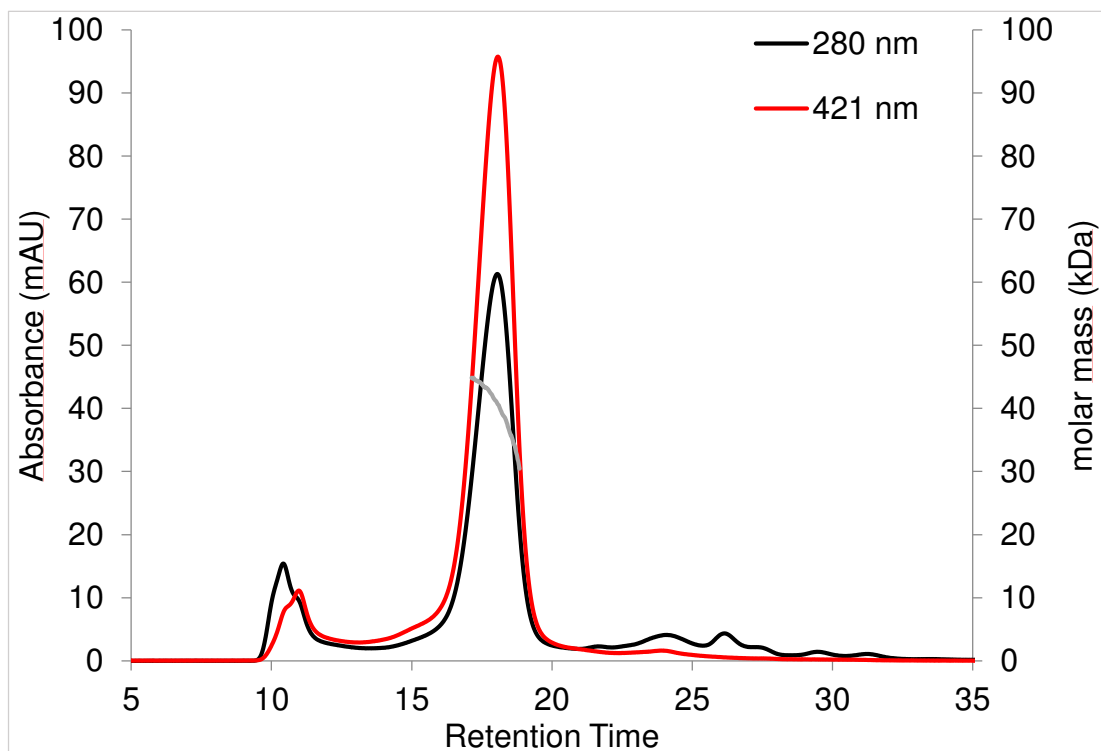


Figure 4-6: Absorbance and molar mass distribution of *An*HTP in relation to the retention time

Figure 4-6 shows the elution profile of *An*HTP, in which the absorbance is plotted against retention time. The absorbance at 421 nm corresponds to the Soret band and the absorbance at 280 nm corresponds to the overall protein absorption. Both absorptions show only one maximum at 18 minutes. This indicates that the protein elutes as a monomer.

The multi angle laser light scattering data, represented by the grey graph, show an average molecular mass of 40.2 kDa. With a theoretical molecular weight of 28.3 kDa, this number would be too high, but considering an average glycosylation of 45 %, which was already proven by the SDS gel, this value fits very well to the monomeric form of the protein. Moreover, the light scattering data show a heterogeneous distribution of the glycosylation. The UV/vis spectrum obtained by the diode array detector at a retention time of 18.1 minutes shows almost identical peaks but has an even better *RZ* value compared to the discussed UV/vis spectrum in chapter 4.4.

With the elution of only one peak, it can be concluded that there is no dimer formation. Apart from very small impurities probably originating from foreign protein, *An*HTP can be considered as pure concerning the HPLC result. Thus, the information about purity and molecular weight obtained from electrophoresis and UV/vis spectrometry could be confirmed by HPLC.

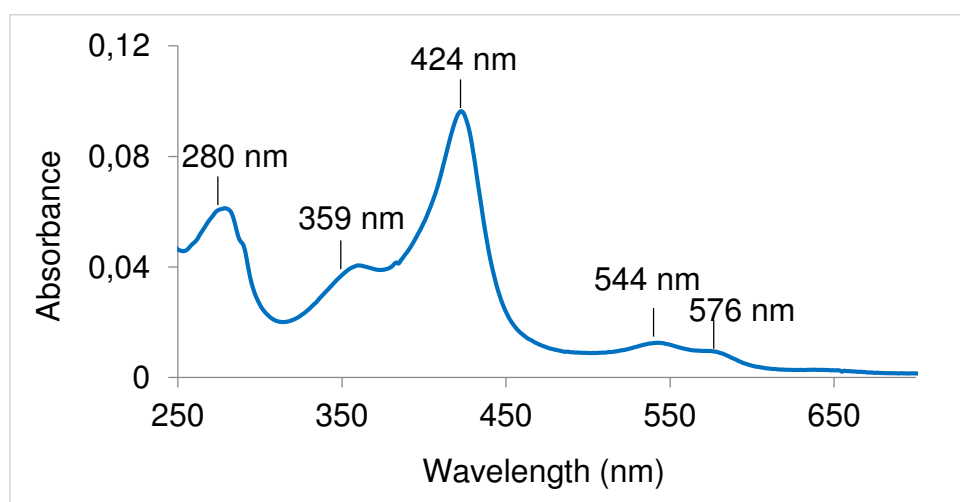


Figure 4-7: UV/vis spectrum of *An*HTP at 18.1 minutes retention time

4.6 pH-dependency of the UV/vis spectrum

This experiment was performed to test whether the UV/vis spectrum of the heme-thiolate peroxygenase undergoes crucial changes in terms of Soret peak shift, electron spin state changes or other modifications with different pH-values. Chloroperoxidase from *Caldariomyces fumago*, a related enzyme from the peroxidase-peroxygenase superfamily (Zámocký *et al.*, 2015) displays crucial spectroscopic changes with altering pH values. Soret peak shifts from 399 nm to 455 nm and also large charge transfer band shifts take place. These changes go together with structural changes of the active center and the heme environment of the enzyme (Hager *et al.*, 1986). To see whether *An*HTP shows similar properties to chloroperoxidase, UV/vis spectra of were measured at varying pH values.

Figure 4-8 shows the spectral transition in the pH range of 2.6 to 7.0. In the acidic pH range, the absorbance of the spectrum is decreasing from pH 7.0 to 4.5. These changes occur mainly in the Soret peak region and the Q band region. Below pH 4.5, the heme peak shifts to lower wavelengths and it gets broader. The spectrum at pH 2.6 is similar to the spectrum of free hemin, which means that the protein denatures under strong acidic conditions and releases heme.

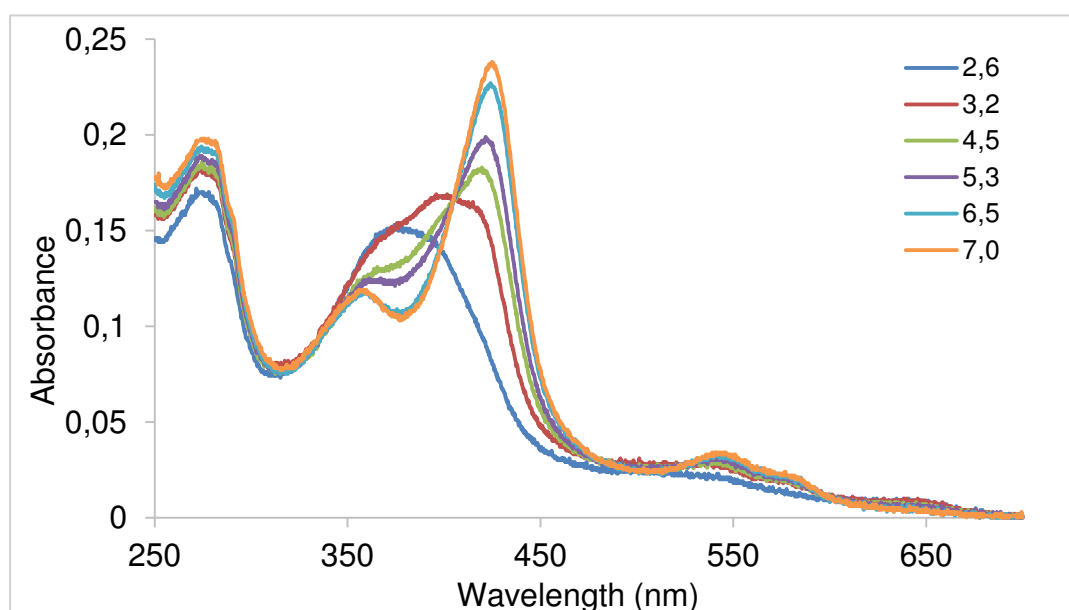


Figure 4-8: UV/vis spectra of *An*HTP at different pH values in the acidic pH range

Similar spectral changes can be found in the basic range (figure 4-9). The absorbance at the Soret region decreases from pH 7.0 to 8.9, above pH 9.0 the protein unfolds and releases heme.

In summary, there is no major change of the UV/vis spectrum with varying the pH values between 4.5 and 8.9. There is no shift in the maximum of the characteristic Soret and Q bands, only a decrease which indicates small structural changes in the heme environment. *An*HTP is structurally stable in a pH range of 4.5 to 8.9. This is in contrast to chloroperoxidase, because CPO shows a very pH-sensitive UV/vis spectrum.

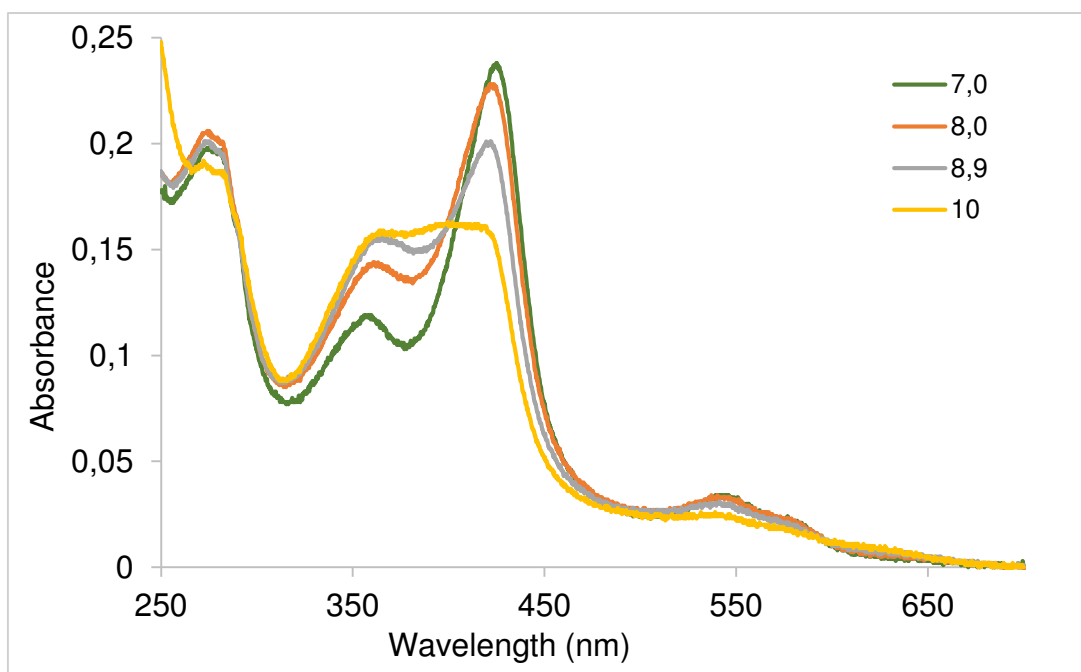


Figure 4-9: UV/vis spectra of *An*HTP at different pH values in the basic pH range

4.7 Reduction with sodium dithionite

The central iron of the heme group in a heme peroxxygenase can have two different oxidation states with different absorption regions, the ferric or iron(III) and the ferrous or iron(II) state. In its resting state, the heme iron of a peroxxygenase is usually in the ferric state. With appropriate reducing

substances, it can be reduced into an iron(II). The experiment was performed to prove if the heme is redox active.

Figure 4-10 shows the spectral transition of *An*HTP (3.6 μ M) upon reduction with 3.9 mM dithionite. The Soret peak shifts 3 nm from 424 to 421 nm and decreases in absorbance upon reduction. Also, the maxima of the Q bands shift from 544 nm and 579 nm to one peak at 551 nm. The δ band at 359 nm vanishes, because the absorption of sodium dithionite superimposes it. However, reduction of the enzyme is possible. Similar spectral transitions can be obtained with other peroxygenases, which confirms that *An*HTP is redox active.

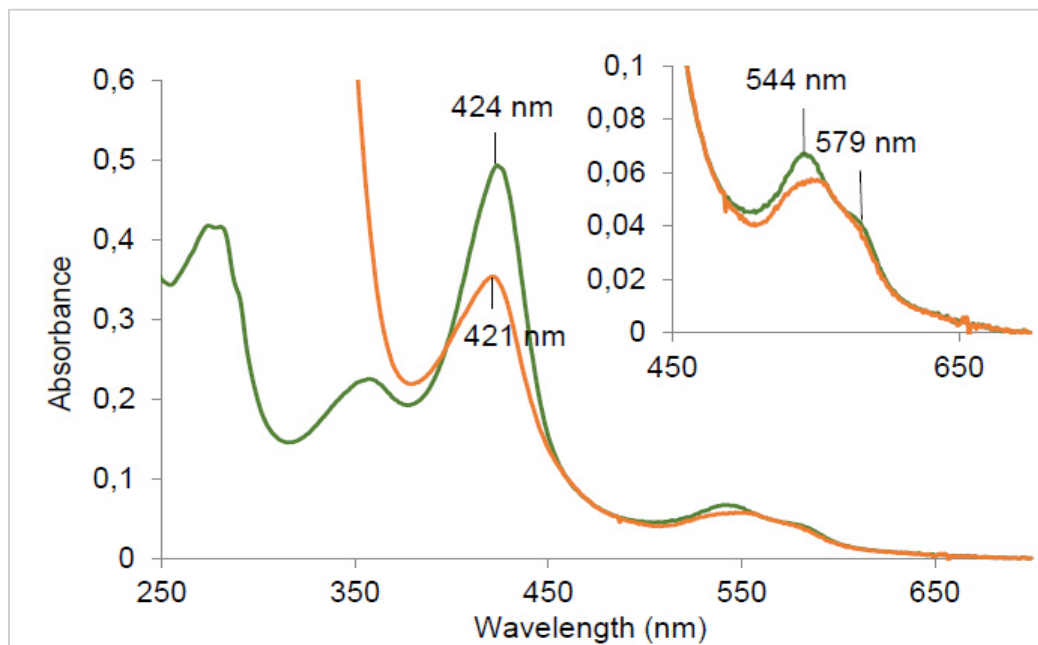


Figure 4-10: Non-reduced (green) and reduced (orange) UV/vis spectrum of *An*HTP

4.8 Steady-state kinetics

Heme-thiolate peroxygenases are versatile biocatalysts, especially concerning H_2O_2 -dependent oxidation reactions like alcohol oxidations, halogenations or sulfoxidations (Pecyna *et al.*, 2010). Therefore, numerous substrates were tested to find out which of the reactions *An*HTP is able to catalyze.

Different substrate concentrations were used, thereby the enzyme concentration was 77 nM, product formation or substrate degradation was followed photometrically.

For the substrates thioanisole and veratryl alcohol, a pH optimum of pH 5.0 was determined (figure 4-11). Activity measurements were performed at this pH. For ABTS, pH 5.0 was used, because under acidic conditions it shows the highest activity.

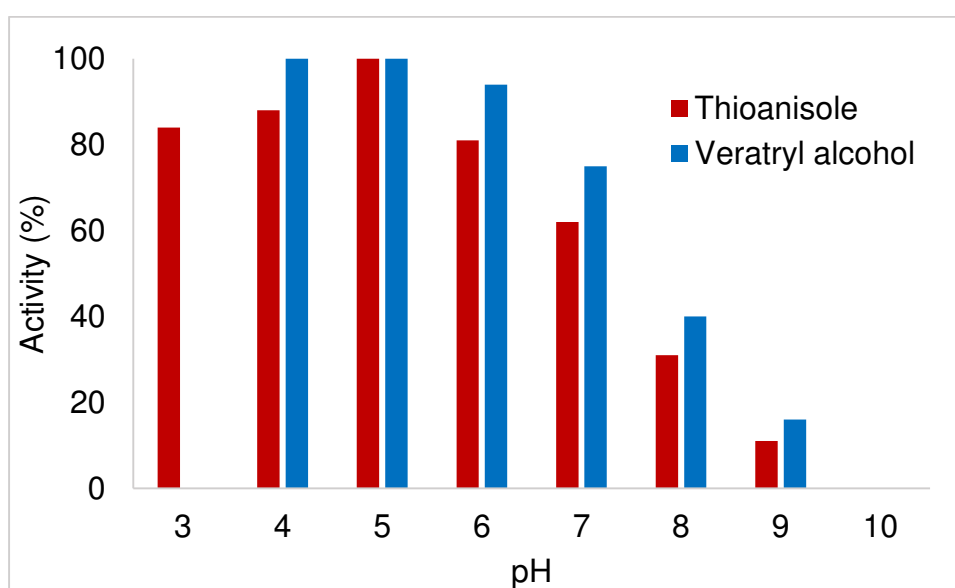


Figure 4-11: Sulfoxidation and alcohol oxidation activity of *An*HTP in % over a pH range of 3 to 10. 100 % are corresponding to 32.7 U/mg and 3.0 U/mg, respectively.

Peroxygenases, and also *An*HTP react according to the so called ping-pong mechanism. The name refers to the alternate binding of substrates and release of products. After binding the first substrate, the first product is released. Then, the second substrate is bound and the second product is released. By transferring a reactive group in this process, an intermediary

enzyme form occurs in the reaction with the first substrate. This reactive group is removed by the second substrate, which results in forming the second product.

All of the following kinetic constants were calculated as shown with ABTS as an example. The initial rate v_0 equals the photometrically determined initial slope of the ABTS oxidation divided by the extinction coefficient of ABTS. Figure 4-12 shows different time traces at 414 nm which were obtained with different ABTS concentrations.

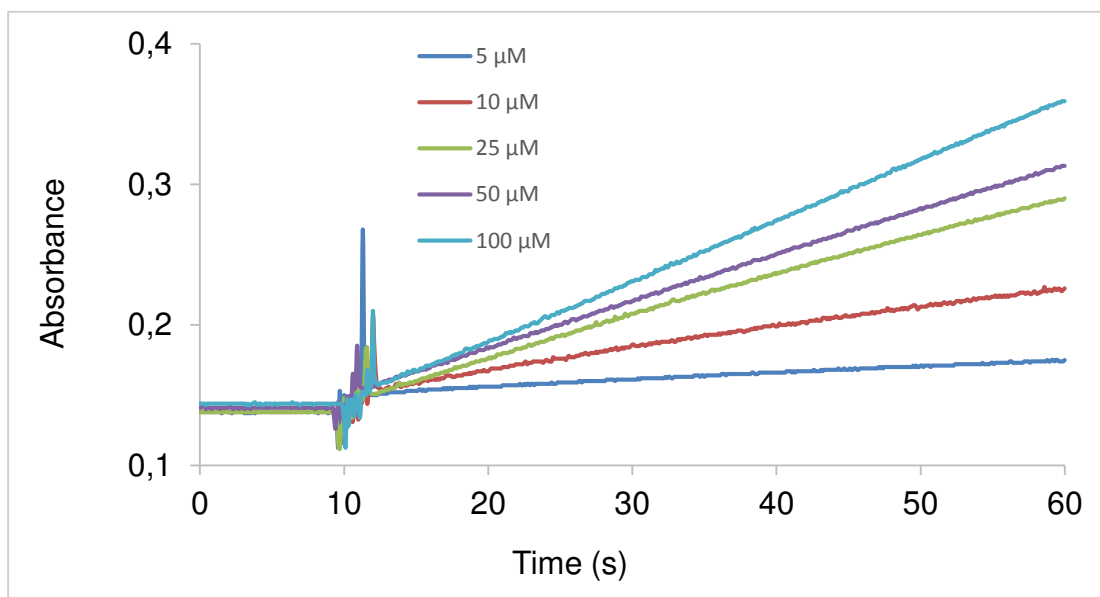


Figure 4-11: Increase of ABTS reaction product absorbance over time

The following calculations and plots are derived from the equation for the forwarding reaction for ABTS:

$$v_0 = \frac{V_1[H_2O_2][ABTS]}{K_M^{H_2O_2}[ABTS] + K_M^{ABTS}[H_2O_2] + [H_2O_2][ABTS]}$$

v_0 : initial rate (μMs^{-1})

V_1 : maximum velocity (μMs^{-1})

$K_M^{H_2O_2}$: Michaelis constant for H_2O_2 (μM)

K_M^{ABTS} : Michaelis constant for ABTS (μM)

$[\text{H}_2\text{O}_2]$: H_2O_2 concentration (μM)

$[\text{ABTS}]$: ABTS concentration (μM)

For the double reciprocal plot, $1/[\text{ABTS}]$ is plotted against $1/v_0$. Compared to other bi-substrate mechanisms, parallel lines are defining the double-reciprocal plot of the ping-pong mechanism.

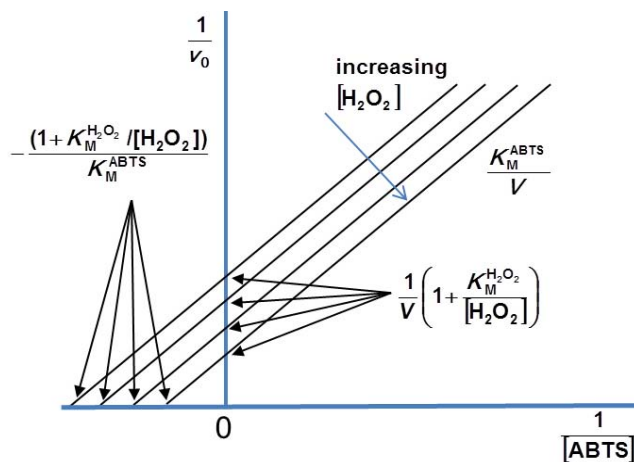


Figure 4-12: Double reciprocal plot

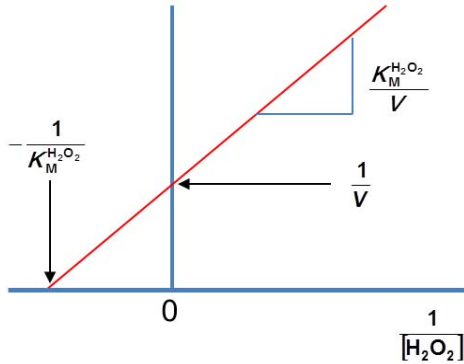
However, with the double reciprocal plot it is not possible to determine the kinetic constants K_M , k_{cat} and k_{cat}/K_M directly. That is why secondary plots are used.

With $1/[\text{H}_2\text{O}_2]$ plotted against the y-intercept of the double reciprocal plot, $K_M^{\text{H}_2\text{O}_2}$ can be calculated. $K_M^{\text{H}_2\text{O}_2}$ is the slope of the straight line divided by V_{max} . With $1/[\text{H}_2\text{O}_2]$ plotted against the x-intercept of the double reciprocal plot, K_M^{ABTS} can be determined. K_M^{ABTS} is the reciprocal of the y-intercept of this secondary plot.

A

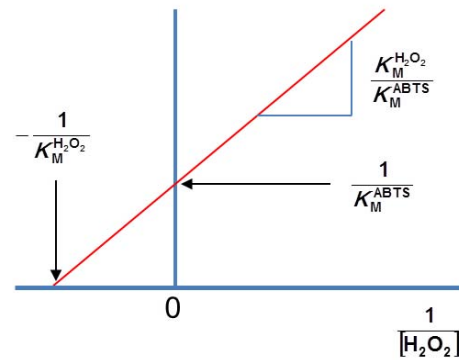
y-intercept =

$$\frac{1}{V} \left(1 + \frac{K_M^{H_2O_2}}{[H_2O_2]} \right) = \frac{1}{V} + \frac{K_M^{H_2O_2}}{[H_2O_2]V}$$

**B**

x-intercept =

$$-\frac{(1 + K_M^{H_2O_2}/[H_2O_2])}{K_M^{ABTS}} = -\frac{1}{K_M^{ABTS}} + \frac{K_M^{H_2O_2}}{K_M^{ABTS}[H_2O_2]}$$

Figure 4-13: Secondary plots for the calculation of K_M values

V_{max} is the reciprocal of the y-intercept of the secondary plots.

k_{cat} is V_{max} divided by the enzyme concentration.

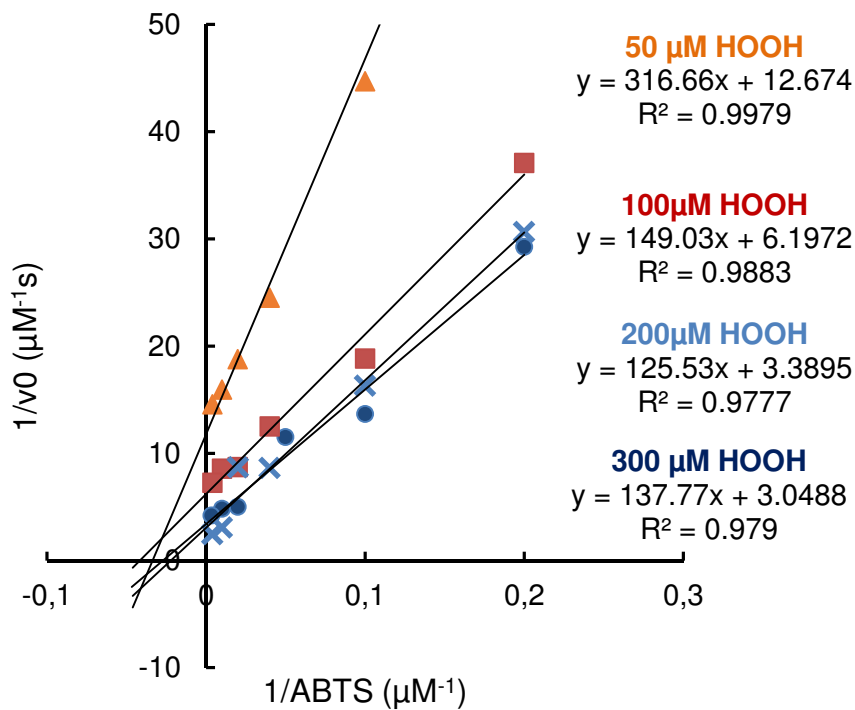


Figure 4-15: Double reciprocal plot for ABTS

Figure 4-15 shows the double reciprocal plot for the ABTS measurements. Characteristic for this plot are parallel lines as shown in figure 4-12. Approximately parallel lines appear for 100 μM , 200 μM and 300 μM H_2O_2 . Only the graph for 50 μM H_2O_2 is not parallel to the other graphs.

Secondary plots of the actually measured values:

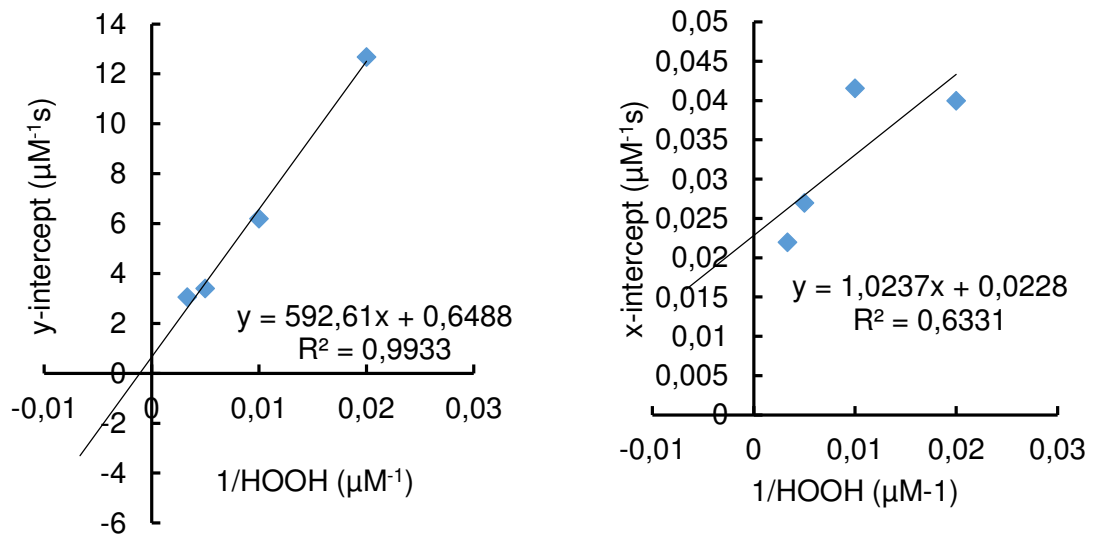


Figure 4-16: Secondary plots for the calculation of K_M values for ABTS and H_2O_2

$$V_{\max} = 1/0.6488 = 1.54 \mu\text{Ms}^{-1}$$

$$k_{\text{cat}} = V_{\max}/C_{\text{enzyme}} = 1.54 \mu\text{Ms}^{-1}/0.0769 \mu\text{M} = 20 \text{ s}^{-1}$$

$$K_M^{\text{H}_2\text{O}_2} = 1.54 \mu\text{Ms}^{-1} \times 592.61 = 913 \mu\text{M}$$

$$K_M^{\text{ABTS}} = 1/\text{intercept} = 1/0.0228 = 44 \mu\text{M}$$

$$k_{\text{cat}} / K_M^{\text{H}_2\text{O}_2} = 2.2 \times 10^5 \text{ M}^{-1} \text{ s}^{-1}$$

$$k_{\text{cat}} / K_M^{\text{ABTS}} = 4.5 \times 10^6 \text{ M}^{-1} \text{ s}^{-1}$$

Table 4-2: Apparent kinetic constants comparison *An*HTP and UPO

Substrate	Kinetic constants	<i>An</i>HTP	UPO *
ABTS	K_M (mM)	0.044	0.05
	k_{cat} (s^{-1})	20	546
	k_{cat}/K_M ($mM^{-1} s^{-1}$)	450	11000
Veratryl alcohol	K_M (mM)	1.3	6.2
	k_{cat} (s^{-1})	2.2	203
	k_{cat}/K_M ($mM^{-1} s^{-1}$)	1.6	32
H_2O_2	K_M (mM)	0.91	1.53
	k_{cat} (s^{-1})	20	676
	k_{cat}/K_M ($mM^{-1} s^{-1}$)	22	442
Thioanisole	K_M (mM)	0.01	none
	k_{cat} (s^{-1})	6.8	none
	k_{cat}/K_M ($mM^{-1} s^{-1}$)	68	none

*Kinetic constants for UPO were taken from Molina-Espeja *et al.*, 2014

Comparing the kinetic constants of *An*HTP and UPO for ABTS is difficult because the Michaelis-Menten parameters were determined at different pH values. The ABTS-activity of UPO was measured at pH 4.0, the pH optimum of the enzyme, whereas the ABTS-activity of *An*HTP was measured at pH 5.0. Nevertheless the substrate affinity, K_M , is almost identical for both enzymes, whereas the turnover number, k_{cat} , of UPO is 27-fold higher. That results in a significantly higher efficiency constant, k_{cat}/K_M , compared to *An*HTP.

The kinetic constants for the other substrates in table 4-2 are directly comparable because they are all measured at pH 5.0. The K_M values of veratryl alcohol are in the same range, but the K_M of *An*HTP is three times smaller which means it has a three times higher substrate affinity compared to UPO. Again, k_{cat} of *An*HTP is almost 200-fold smaller than the turnover number of UPO, which leads to a 20-fold higher k_{cat}/K_M for UPO. Roughly the same statement can be made about the Michaelis-Menten parameters for H_2O_2 . The substrate binds in approximately the same affinity to the enzyme, but k_{cat} and k_{cat}/K_M of *An*HTP are 30 times and 20 times lower, respectively. The crucial statement of these measurements is that both enzymes bind the

substrate equally strong, but the turn over number of *An*HTP is always lower. A possible explanation for this fact could be that the catalysis in both enzymes is different.

Sulfoxidation of *An*HTP was measured with thioanisole. Compared to the other substrates of *An*HTP, the substrate affinity of thioanisole is the highest, due to the lowest K_M value. The turnover number and k_{cat}/K_M values are in the middle range.

Chloroperoxidase shows some catalase activity, therefore we also measured the catalase activity of *An*HTP, but we could not determine any activity. From other heme-thiolate peroxygenases it is known that they catalyze alcohol oxidation and bromination reactions thus these reactions were also tested with *An*HTP using vanillyl alcohol and taurine respectively. Heme-thiolate peroxygenase of *Aspergillus niger* shows some alcohol oxidation activity with veratryl alcohol, but not with vanillyl alcohol as well as it does not show any bromination activity.

4.9 Sodium cyanide titration

With cyanide binding, information about the accessibility of the active center of heme peroxidases can be obtained. Cyanide enters the distal heme cavity and binds tightly to the iron(III) of the heme, which results in the conversion of the high-spin to a low-spin electron state and causes the red-shift of the Soret-band in the UV/vis spectrum.

The absorbance changes of the heme-thiolate peroxygenase of *Aspergillus niger* with sodium cyanide are rather small as shown in figure 4-17:

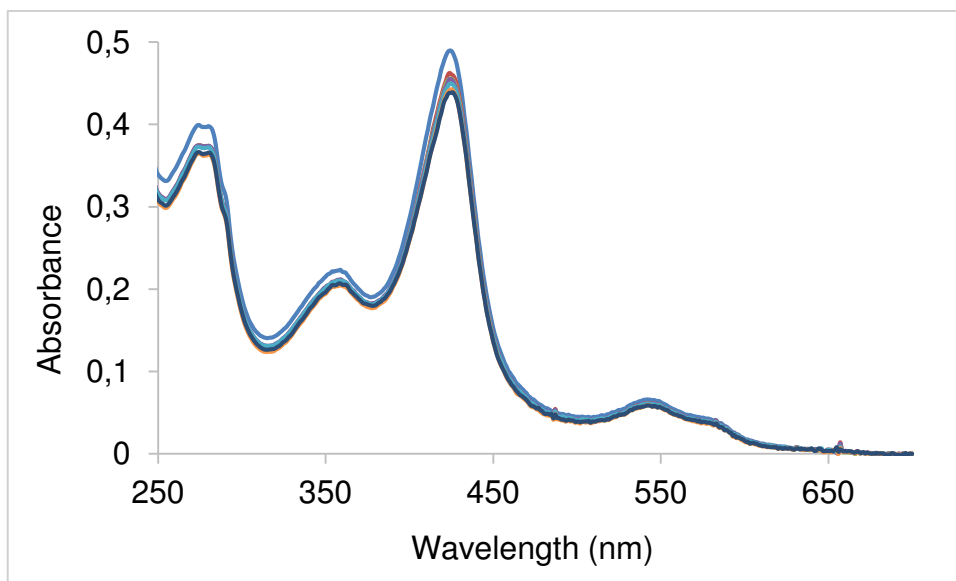


Figure 4-17: UV/vis spectra of AnHTP with increasing sodium cyanide concentrations (1.0 μM , 2.0 μM , 3.0 μM , 4.0 μM , 5.0 μM , 6.0 μM , 8.4 μM , 11 μM , 17 μM , 23 μM)

The heme peak was 2 nm red-shifted from 424 nm to 426 nm with increasing sodium cyanide concentration from 1 to 23 μM . Enzyme concentration was 3.6 μM . Additionally, with increasing cyanide concentration, the absorbance of the Soret peak was slightly decreasing.

Plotting the absorbance differences in the Soret peak at 424 nm against the cyanide concentration in (μM), the dissociation constant, K_d , can be determined by fitting the data with a rectangular hyperbolic function (figure 4-18). K_d was determined to be 4.6 μM which means that cyanide binds very tightly to the central iron of the heme.

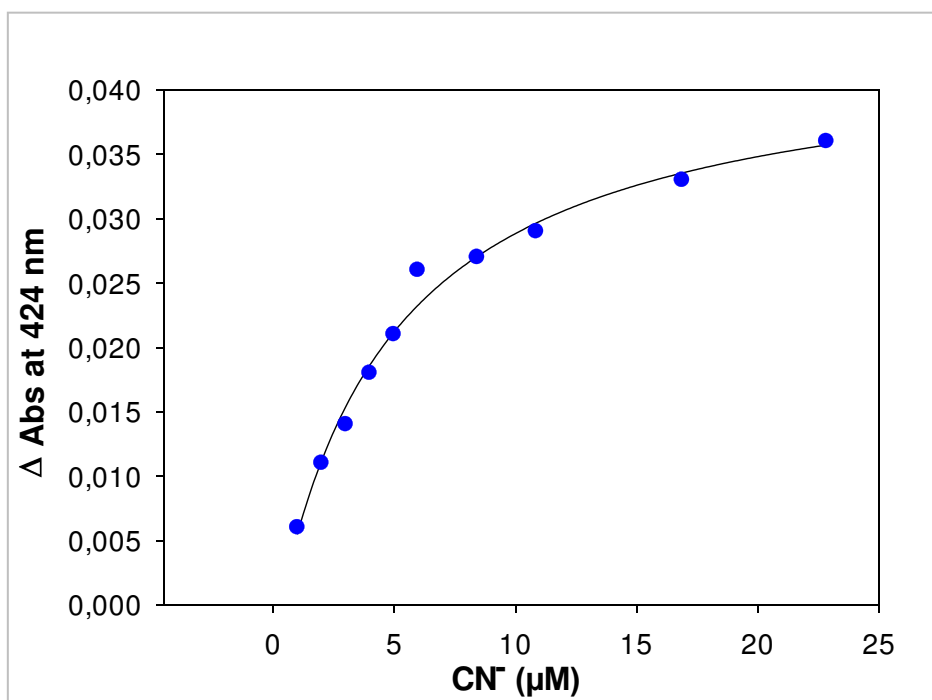


Figure 4-18: Absorbance differences at 424 nm plotted against increasing sodium cyanide concentrations

UV/vis spectra of heme peroxygenases are usually more red-shifted upon cyanide binding than in the case of *An*HTP, because of inducing a low-spin complex. For example the Soret peak shift of chloroperoxidase is 18 nm from 421 nm to 439 nm compared to the 2 nm shift of *An*HTP. With 19 μM however, the K_d value of chloroperoxidase is in a similar range (Hager *et al.*, 1986) than the K_d value of 4.6 μM of *An*HTP. This indicates a similar accessibility and similar strong binding behavior of cyanide to the heme iron of both enzymes.

4.10 Circular Dichroism

Circular dichroism was used to measure the temperature stability of the enzyme in the far UV and visible range. Temperature stability is expressed by the T_m value. The T_m value is the melting temperature and is defined as the temperature where half of the protein is folded and half of it is unfolded. Moreover, a CD measurement in the Far UV region between 190 nm and 250 nm allows making a prediction of the secondary structure composition of the investigated protein. The measurements were performed with an enzyme

concentration of 3.6 μM and in a 10 mM sodium phosphate buffer pH 7.0. The heating rate was 1 $^{\circ}\text{C}$ per minute.

The circular dichroism spectrum of *An*HTP was measured at 20 $^{\circ}\text{C}$ and at 90 $^{\circ}\text{C}$:

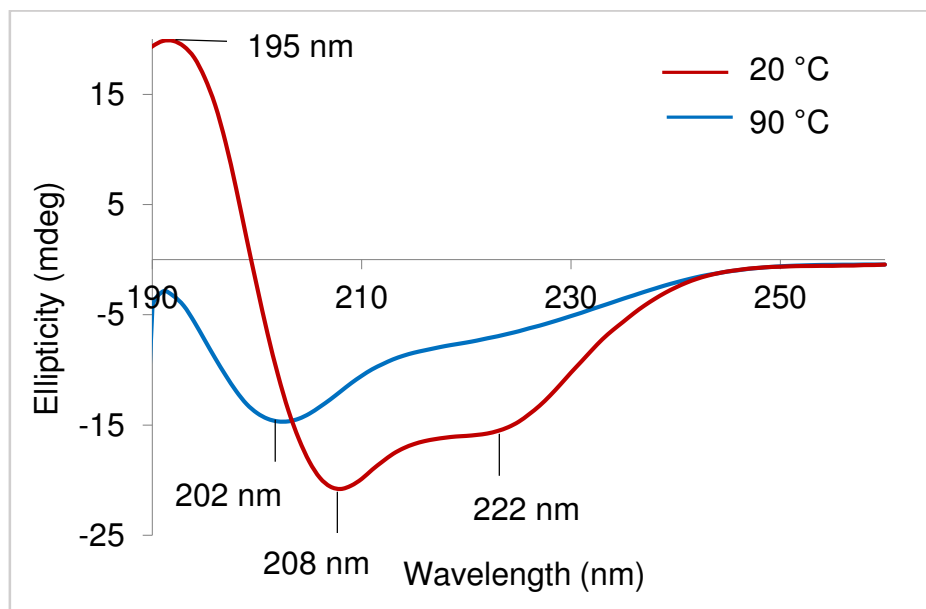


Figure 4-19: CD spectra of *An*HTP at 20 $^{\circ}\text{C}$ (red) and 90 $^{\circ}\text{C}$ (blue)

Figure 4-19 shows the overlay of the far UV CD spectra at 20 and 90 $^{\circ}\text{C}$. The far UV spectrum at 20 $^{\circ}\text{C}$ shows two minima at 208 nm and 222 nm and a maximum at 195 nm, which is consistent with a mainly α -helical protein. At 90 $^{\circ}\text{C}$ the protein is mainly unfolded, and consists primarily of random coils.

The table 4-3 below shows the secondary structure composition of *An*HTP at 20 $^{\circ}\text{C}$, which was calculated with the program CDNN:

Table 4-3: Secondary structure composition of *An*HTP in %

	190 - 260 nm
Helix	33,63%
Antiparallel	10,02%
Parallel	8,07%
Beta-Turn	17,20%
Rndm. Coil	29,25%
Total Sum	98,15%

*An*HTP is composed of 34% α -helices, 18% β -sheets, 17% β -turn and 29% random coils.

A temperature curve from 20 °C to 90 °C was measured to test the temperature stability in the far UV range. Figure 4-20 shows the thermal transition of *An*HTP recorded at 222 nm.

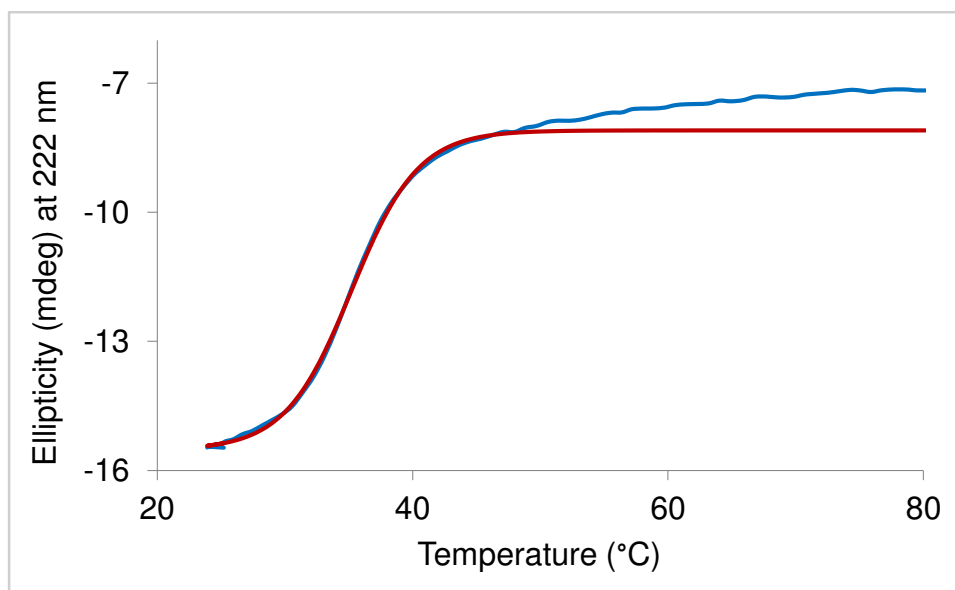


Figure 4-20: Temperature-mediated unfolding of *An*HTP at 222 nm, sigmoid fit (red)

With a sigmoid fit of the curve, a T_m value of 35.2 °C, which is located in the center of the transition area, was calculated.

Figure 4-21 shows the CD spectrum of *An*HTP in the near UV and visible range. The spectrum shows two minima (286 nm, 298 nm) in the near UV where the aromatic amino acids absorb and one minimum in the visible range at 431 nm where we can get information about the heme environment.

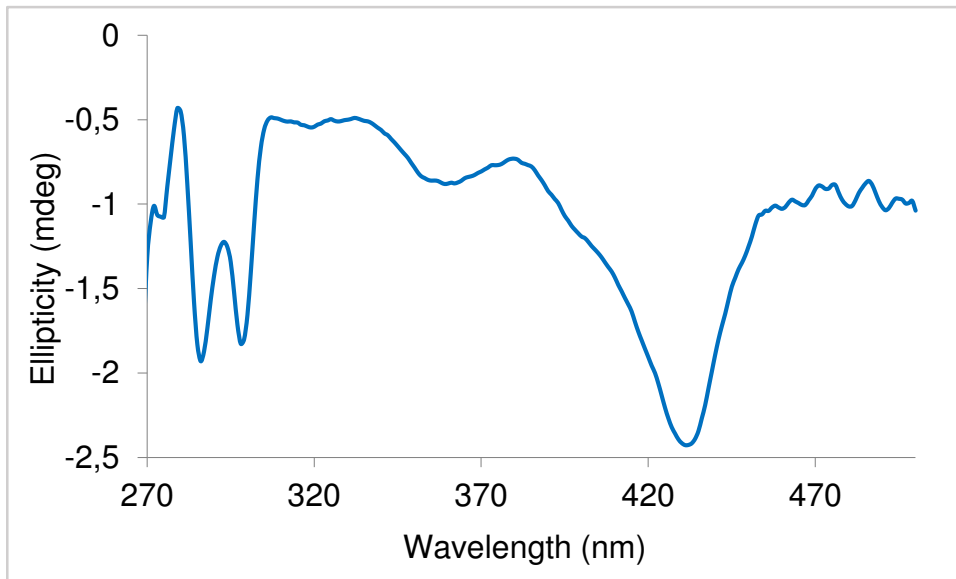


Figure 4-21: CD spectrum of AnHTP in the visible region

Figure 4-22 shows the corresponding temperature curve at 431 nm. The data could be fitted with a sigmoid fit, resulting in a T_m value of 36.6 °C.

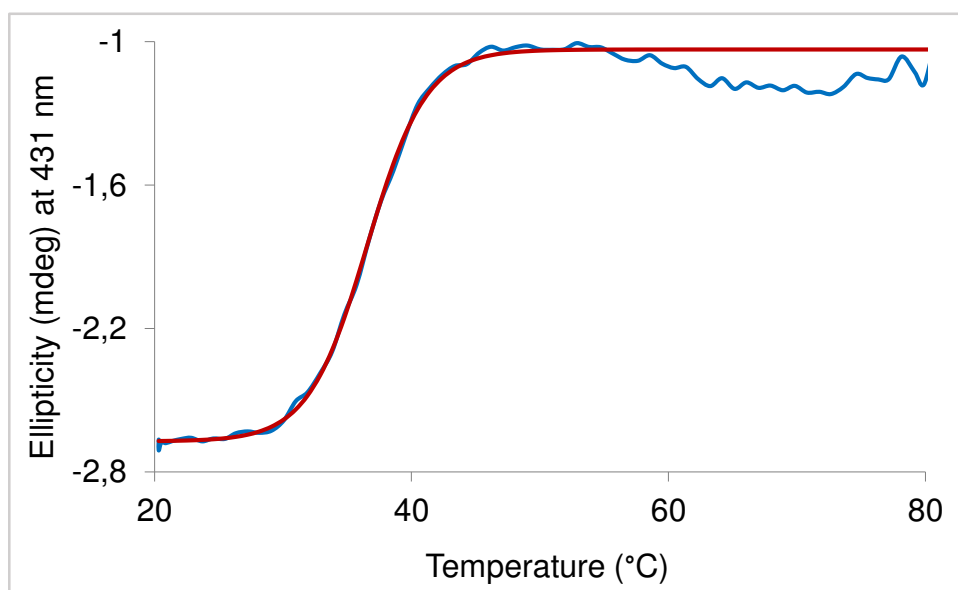


Figure 4-22: Temperature-mediated unfolding of the active center of AnHTP at 431 nm, sigmoid fit (red)

From the temperature curves in figures 4-20 and 4-22 it can be said, that the unfolding is completed at approximately 40 °C. There is one transition and therefore one major unfolding event in both the secondary structure region and

in the heme region. The T_m value at 222 nm (35.2 °C) corresponds to the unfolding of the secondary structure, whereas the T_m value at 431 nm (36.6 °C) corresponds to the unfolding of the active site and the release of the heme. Both values are rather similar, which indicates that the secondary structure and the heme environment unfold simultaneously.

Secondary structure composition of *An*HTP is different to UPO. Every kind of secondary structure - α -helices, β -structures and random coils - in *An*HTP is represented by one third, whereas UPO has twice as much α -helices than β -sheets (Piontek *et al.*, 2013). The T_m value for the unspecific peroxygenase of *Agrocybe aegerita* is 52.3 °C (Molina-Espeja *et al.*, 2014), which is significantly higher than the T_m values for *An*HTP. Normally fungal heme-thiolate peroxygenases are extracellular enzymes, and they are usually very stable (Hofrichter *et al.*, 2014). Interestingly, this is not the case for *An*HTP, which has low T_m values and therefore a low temperature stability.

4.11 Differential Scanning Calorimetry

The thermal stability was also tested with Differential Scanning Calorimetry (DSC). The thermogram was baseline corrected and fitted with a non-two-state transition model. The protein concentration was 7.2 μ M and a 10 mM phosphate buffer pH 7.0 was used. The temperature range was 20 °C to 100 °C and the heating rate was 1 °C per minute.

The thermogram in figure 4-23 shows two endotherms, one at 38.3 °C and a small one at 51.5 °C. With CD, melting temperatures similar to $T_m 1 = 38.3$ °C could be obtained: 35.2 °C in the far UV region and 36.6 °C in the visible range. This confirms that *An*HTP has a low temperature stability. The appearance of $T_m 2$ cannot be explained without further investigation.

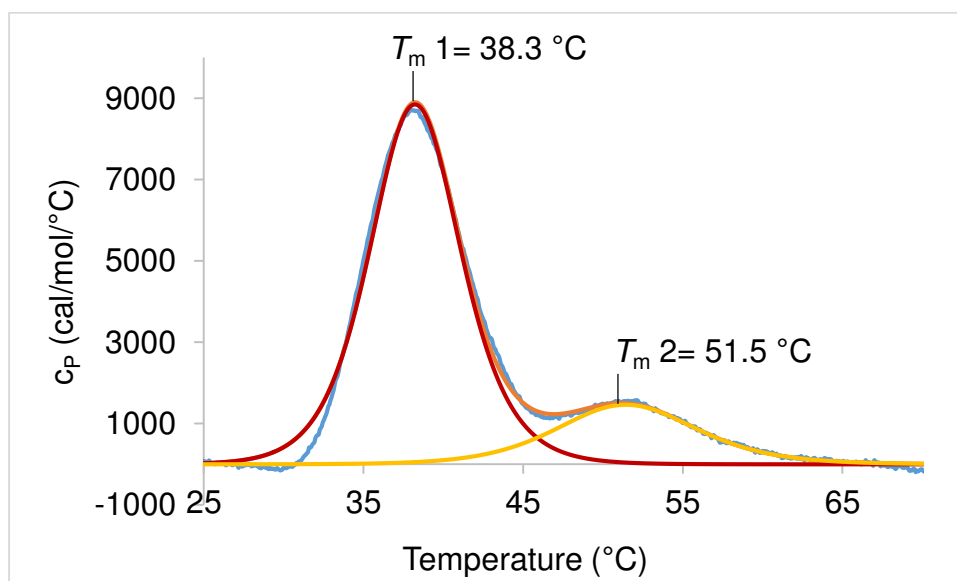


Figure 4-23: Differential scanning calorimetry thermogram of AnHTP

4.12 Stopped-flow spectroscopy

The stopped-flow experiment was performed to analyze compound I formation with *meta*-chloroperoxybenzoic acid (mCPBA). In this reaction, mCPBA is reduced in a two electron reaction to its corresponding aldehyde, which is shown in figure 4-24 (Wang *et al.*, 2015). The resting state of the enzyme is thereby converted into an oxidized intermediate called compound I, that is an oxoiron(IV) porphyrin radical cation (Wang *et al.*, 2012).

The enzyme concentration was 2.4 μM , the substrate concentration was varied between 25 μM and 70 μM and the conventional stopped-flow mode was used for the measurement.

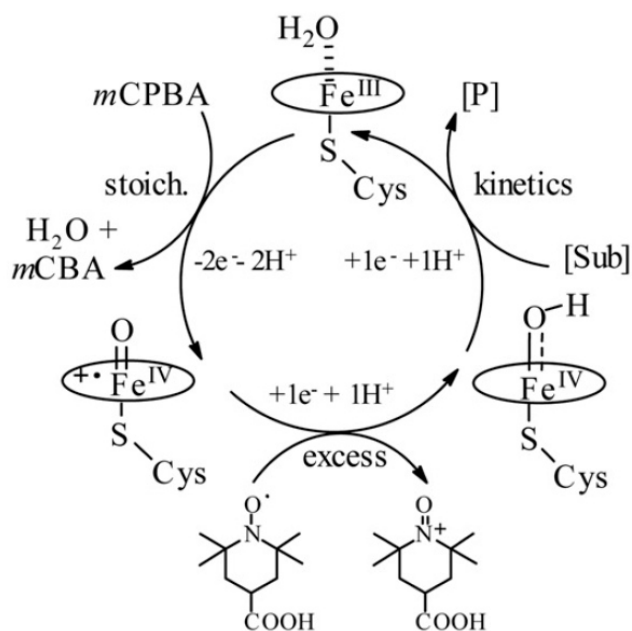


Figure 4-24: Proposed reaction scheme for oxidation of *AnHTP* by *meta*-chloroperoxybenzoic acid (Wang *et al.*, 2015)

Compound I can be distinguished from the native form of the enzyme by its reduced absorbance in the Soret region. The transition of native *AnHTP* with 50 μM *mCPBA* (figure 4-25) shows a more than 50% decrease in heme absorbance at 425 nm. At 506 nm, an isosbestic point can be detected. This means, there is a direct transition of ferric *AnHTP* to compound I without any intermediate. The spectral changes occurred within 6.5 s after mixing enzyme and substrate.

At 425 nm, the most significant changes in absorbance occurred during the formation of compound I. At this wavelength the transition was biphasic. Figure 4-26 shows, the absorbance change of native *AnHTP* with 50 μM *mCPBA* within 10 s. With a double-exponential fit, the pseudo-first-order rate constants $k_{\text{obs}(1)}$ and $k_{\text{obs}(2)}$ could be determined.

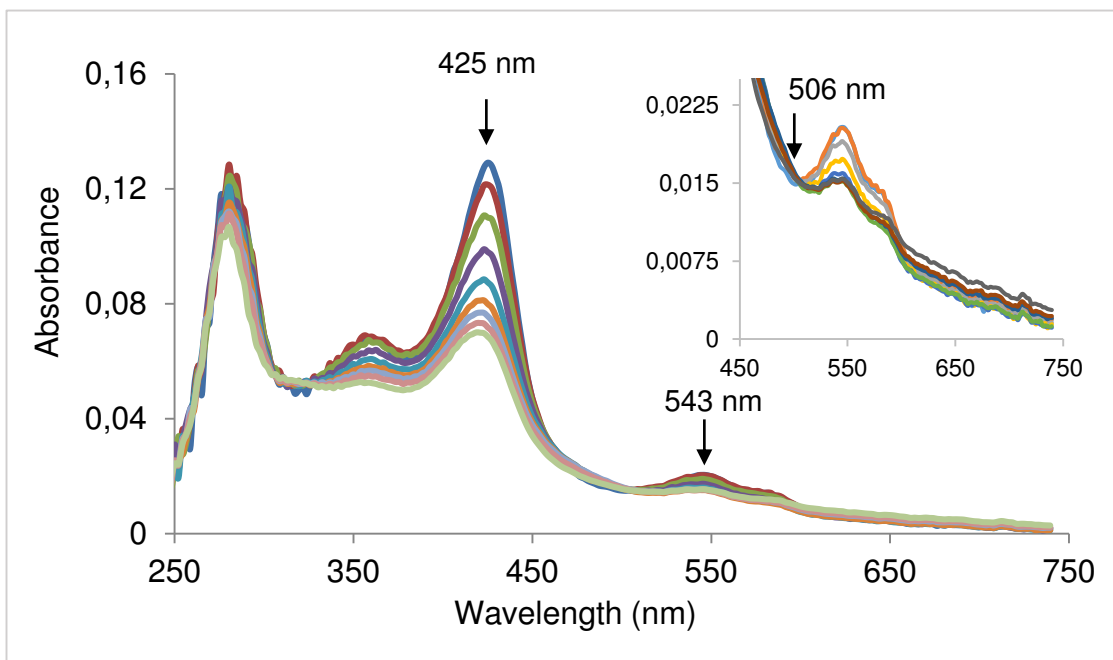


Figure 4-25: Reaction of *AnHTP* with *m*-CPBA, spectra recorded after 0.005 s, 0.066 s, 0.136 s, 0.317 s, 0.561 s, 0.947 s, 1.56 s, 3.53 s, 6.51 s. The arrows show the decrease of absorbance with time at a specific wavelength.

Plotting $k_{\text{obs}(1)}$ against the measured substrate concentrations the apparent second-order rate constant, k_{app} , can be obtained from the slope of the linear plot (figure 4-27). k_{app} was $3.5 \times 10^4 \text{ M}^{-1} \text{ s}^{-1}$ at pH 7.0 and it represents the rate constant of the first main absorbance change, the compound I formation. $k_{\text{obs}(2)}$ corresponds to the second small absorbance change which is not dependent on the *m*CPBA concentration.

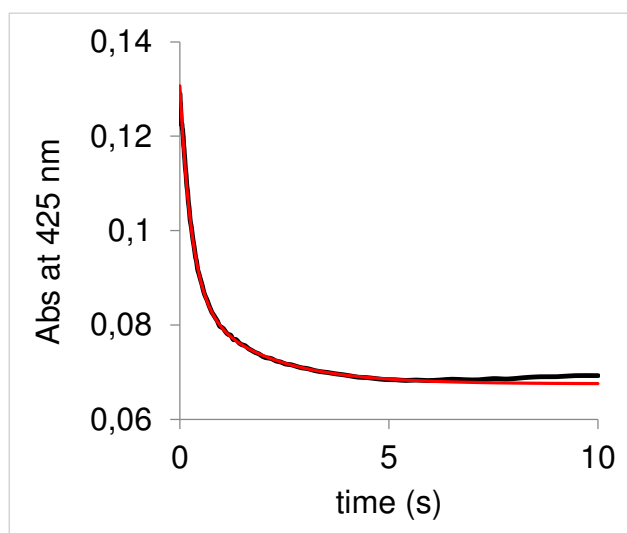


Figure 4-26: Double exponential fit (red) of change of absorbance at 425 nm over time

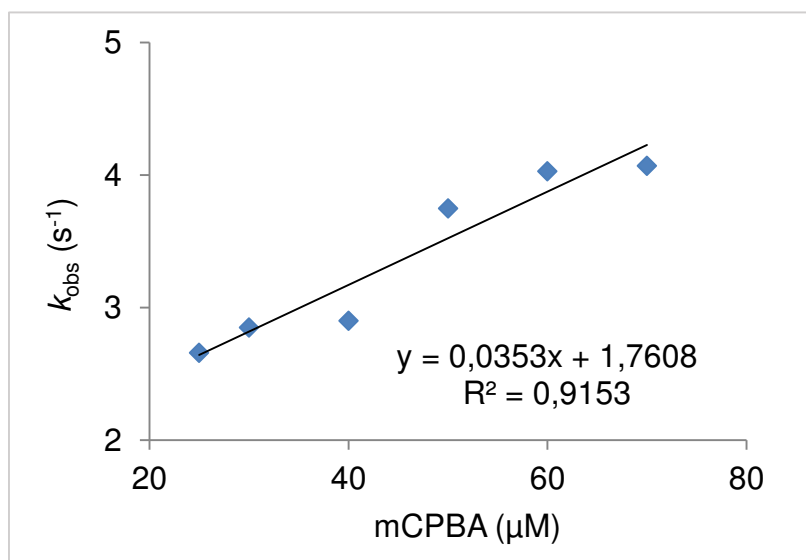


Figure 4-27: k_{obs} in relation to different substrate concentrations, k_{app} can be obtained from the slope of the linear fit

Comparing the results of *An*HTP with UPO of *Agrocybe aegerita*, the resting state spectrum of the UPO shows a Soret maximum at 417 nm and two Q bands at 538 nm and 571 nm, indicating a low-spin state which is similar to *An*HTP. *An*HTP also shows a low-spin state with a Soret maximum at 424 nm and two Q bands at 544 nm and 579 nm. The decrease of the heme peak of both enzymes is significant. Moreover, *An*HTP as well as UPO has at least one isosbestic point, demonstrating a direct transition to compound I. In contrast to *An*HTP, UPO compound I displays additional peaks at 361 nm and 694 nm. Also, the Soret band of UPO is blue shifted and the absorbance changes at 694 nm leading to the conclusion of the presence of compound I. The apparent second-order rate constant for UPO compound I formation is $1.1 (\pm 0.5) \times 10^7 \text{ M}^{-1} \text{ s}^{-1}$ at pH 6.0 (Wang et al., 2012), which is significantly faster than the reaction of *An*HTP with *m*CPBA.

5 Conclusion

The expression and purification of heme-thiolate peroxygenase from *Aspergillus niger* was carried out successfully. A sufficient amount of protein could be expressed in *Pichia pastoris* within few days. This was followed by a simple purification protocol consisting of ammonium sulfate precipitation and a metal chelate affinity chromatography step. The resulting yield was 2.8 mg/L and the *Reinheitszahl* was 1.2. With further expression screenings and changing parameters of the expression protocol like incubation temperature or hemin concentration, the yield could probably be increased to yields (217 mg/L) which was published by Molina-Espeja *et al.* 2015 for UPO. Another possibility would be to produce the enzyme in a bioreactor by upscaling.

The main focus of the thesis was to characterize the peroxygenase from *Aspergillus niger* and compare it to chloroperoxidase and unspecific peroxygenase. The spectral properties of AnHTP are very similar to those of UPO and CPO. The glycosylation degree is also comparably high and the molecular weight approximately fits into the usual range of 32 to 46 kDa for peroxidase-peroxygenases (Hofrichter *et al.*, 2014). The UV/vis spectrum of AnHTP is barely dependent of the pH-value. There is only a slight decrease of the heme peak in between pH 4.5 and 8.9, which means that the enzyme is stable in this range. Below and above those values, it denatures and releases the heme. In contrast to that, CPO shows major pH-dependent heme peak shifts. Furthermore, the enzyme can be reduced, the Soret peak is blue shifted, that means, that the peroxygenase is redox active. The UV/vis spectrum of AnHTP indicates a low-spin state of the heme iron. But to elucidate the true heme coordination, further experiments like electron spin resonance measurements would be necessary. Cyanide binding shows accessibility of the heme cavity and a similarly strong binding behavior than chloroperoxidase.

Temperature stability was measured with circular dichroism and differential scanning calorimetry. Both measurements showed an almost identical unfolding process with a single unfolding event. The unfolding of the secondary structure and the unfolding of the active site occur at the same

temperature. With an average T_m value of 37 °C, *An*HTP has a rather low temperature stability, especially when compared to UPO ($T_m = 52.3$ °C). Circular dichroism also gives information about the secondary structure. *An*HTP consists of one third α -helices, one third β -structures and one third random coils. UPO however is composed of twice as much α -helices as β -sheets (Piontek *et al.*, 2013).

Temperature stability of *An*HTP would be a crucial point for genetic engineering. To achieve a proper working enzyme for industrial purposes, it needs to be more stable at higher temperatures.

The enzyme has peroxidase activity with ABTS, sulfoxidation activity with thioanisole and alcohol oxidation activity with veratryl alcohol. pH optimum measurements show that the enzyme prefers an acidic environment. Steady-state kinetics show that both *An*HTP and UPO have similarly high binding affinities to the above mentioned substrates, but the latter has significantly higher turnover numbers (Molina-Espeja *et al.*, 2014).

Compound I formation of *An*HTP could be demonstrated with *m*CPBA, but the apparent rate constant is much lower compared to that for UPO (Wang *et al.*, 2012).

Heme-thiolate peroxygenase of *Aspergillus niger* could be expressed, purified and characterized to a satisfying extent. But there are many questions open. At first, it would be desirable to find the natural substrate of *An*HTP. Also, additional substrates need be tested with regard to oxyfunctionalization. compound II formation is a further task to be coped with. Genetic engineering concerning temperature stability and enzyme activity as well as substrate variability are next steps towards a more efficient industrial applicable enzyme. Expression needs to be optimized by varying culture conditions, and purification can be complemented by size exclusion chromatography. The structure also needs to be elucidated. Electron-spin resonance spectroscopy could give an insight into the active center and the spin-state of heme, and a solved crystal structure could contribute to elucidate the catalytic mechanism of the enzyme.

6 References

- Bordeaux M., Galarneau A., Drone J., (2012) Catalytic, Mild and Selective Oxyfunctionalization of Linear Alkanes: Current Challenges. *Angew Chem Int Ed Engl.*, 51(43):10712-23.
- Bormann S., Baraibar A. G., Ni Y., Holtmann D., Hollmann F., (2015) Specific oxyfunctionalisations catalysed by peroxygenases: opportunities, challenges and solutions. *Catal. Sci. Technol.*, 5, 2038-2052.
- Hofrichter M., Ullrich R., Pecyna M.J., Liers C., Lundell T., (2010) New and classic families of secreted fungal heme peroxidases. *Appl Microbiol Biotechnol*, 87:871-897.
- Hofrichter M., Ullrich R., (2014) Oxidations catalyzed by fungal peroxygenases. *Cur. Opinion Chem. Biol.*, 19:116-125.
- Kühnel K., Blankenfeldt W., Terner J., Schlichting I., (2006) Crystal Structures of Chloroperoxidase with Its Bound Substrates and Complexed with Formate, Acetate and Nitrate. *J. Biol. Chem.*, 281, 33, 23990-23998.
- Molina-Espeja P., Garcia-Ruiz E., Gonzalez-Perez D., Ullrich R., Hofrichter M., Alcalde M., (2014) Directed Evolution of Unspecific Peroxygenase from *Agrocybe aegerita*. *Appl. and Environ. Microbiol.* 80, 11, 3496-3507.
- Molina-Espeja P., Ma S., Mate D.M., Ludwig R., Alcalde M., (2015) Tandem-yeast expression system for engineering and producing unspecific peroxygenase. *Enzyme and Microbial Technology*, 73-74 29-33.
- Morris D. R., Hager L. P., (1966) Chloroperoxidase – Isolation and Properties of the chrySTALLINE Glycoprotein. *J. Biol. Chem.*, 241, 8, 1763-1768.
- Pecyna M. J., Ullrich R., Bittner B., Clemens A., Scheibner K., Schubert R., Hofrichter M., (2010) Molecular characterization of aromatic peroxygenase from *Agrocybe aegerita*. *Appl Microbiol Biotechnol.*, 84(5):885-97.
- Piontek K., Strittmatter E., Ullrich R., Gröbe G., Pecyna M.J., Kluge M., Scheibner K., Hofrichter M., Plattner D.A. (2013) Structural Basis of Substrate Conversion in a New Aromatic Peroxygenase. *J. Biol. Chem.*, 288, 48, 34767-34776.
- Reetz M. T., (2013) Biocatalysis in Organic Chemistry: Past, Present and Future. *J. Am. Chem. Soc*, 135, 12480–12496.
- Sono M., Dawson J. H., Hall K., Hager L. P., (1986) Ligand and Halide Binding Properties of Chloroperoxidase: Peroxidase-Type Active Site Heme Environment with Cytochrome P-450 Type Endogenous Axial Ligand and Spectroscopic Properties. *Biochemistry*, 25, 347-356.
- Sundaramoorthy M., Terner J., Poulos T. L., (1995) The crystal structure of chloroperoxidase: a heme peroxidase-cytochrome P450 functional hybrid. *Structure*, 3(12):1367-77.

- Wang X., Peter S., Kinne M., Hofrichter M., Groves J. T., (2012) Detection and Kinetic Characterization of a Highly Reactive Heme-Thiolate Peroxygenase Compound I. *J. Am. Chem. Soc.*, 134(31): 12897-12900.
- Wang X., Ullrich R., Hofrichter M., Groves J. T., (2015) Heme-thiolate ferryl of aromatic peroxygenase is basic and reactive. *PNAS*, 112, 12, 3686-3691.
- Weiss S.J., Klein R., Slivka A., Wei M., (1982) Chlorination of Taurine by Human Neutrophils. *J. Clin. Invest.*, 70:598-607.
- Zámocký M., Gasselhuber B., Furtmüller P. G., Obinger C., (2012) Molecular evolution of hydrogen peroxide degrading enzymes. *Arch Biochem Biophys.* 525(2): 131–144.
- Zámocký M., Hofbauer S., Schaffner I., Gasselhuber B., Nicolussi A., Soudi M., Pirker K. F., Furtmüller P. G., Obinger C., (2015) Independent evolution of four heme peroxidase superfamilies. *Archives of Biochemistry and Biophysics*, 574:108-19.